Focal and Systemic Immune Responses Following Intracerebral Hemorrhage

by

Samuel Xiang-Yu Shi

A Dissertation Presented in Partial Fulfillment
of the Requirements for the Degree
Doctor of Philosophy

Approved November 2020 by the
Graduate Supervisory Committee:

Yung Chang, Chair
Rayna J. Gonzales
Andrew F. Ducruet
Qiang Liu

ARIZONA STATE UNIVERSITY

December 2020

ABSTRACT

Intracerebral hemorrhage (ICH) is a devastating type of acute brain injury with high mortality and disability. Acute brain injury swiftly alters the immune reactivity within and outside the brain; however, the mechanisms and influence on neurological outcome remains largely unknown. My dissertation investigated how ICH triggers focal and systemic immune responses and their impact hemorrhagic brain injury. At the focal level, a significant upregulation of interleukin (IL)-15 was identified in astrocytes of brain sections from ICH patients. A transgenic mouse line where the astrocytic IL-15 expression is controlled by a glial fibrillary acidic protein promoter (GFAP-IL-15^{tg}) was generated to investigate its role in ICH. Astrocyte-targeted expression of IL-15 exacerbated brain edema and neurological deficits following ICH. Aggravated ICH injury was accompanied by an accumulation of pro-inflammatory microglia proximal to astrocytes in perihematomal tissues, microglial depletion attenuated the augmented ICH injury in GFAP-IL-15^{tg} mice. These findings suggest that IL-15 mediates the crosstalk between astrocytes and microglia, which worsens ICH injury.

Systemic immune response was investigated by leveraging the novel method of obtaining and analyzing bone marrow cells from the cranial bone flaps of ICH patients. A swift increase of hematopoietic stem cell (HSCs) population in the bone marrow was identified, along with a shift towards the myeloid cell lineage. Human findings were mirrored in an ICH mouse model. Fate mapping these HSCs revealed increased genesis of Ly6C^{low} monocytes in the bone marrow, which transmigrate into the hemorrhagic brain and give rise to alternative activation marker bearing macrophage. Blockade of the β3-adrenergic receptor or inhibition of Cdc42 abolished ICH-induced myeloid bias of HSCs. Importantly, mirabegron, a Food and Drug Administration-approved β3 adrenergic receptor agonist, and a Cdc42 activator, IL-3, enhanced bone marrow generation of Ly6C^{low} monocytes and improved recovery. These results suggest that brain injury modulates HSC lineage destination to curb distal brain inflammation, implicating the bone marrow as a unique niche for self-protective neuroimmune interactions. Together, these results

demonstrate how acute brain injury exerts a profound yet distinct effect on immune responses within and outside the brain and sheds new light on neuroimmune interactions with potential clinical implications.

Key words: intracerebral hemorrhage, inflammation, immunity, stroke, immune modulation

ACKNOWLEDGEMENTS

The completion of this dissertation was supported by many individuals. Foremost, I must extend my gratitude to my advisory committee, their generosity with time and expertise were crucial for my development as a research scientist throughout the duration of my graduate education. Dr. Chang, who chaired my committee, was instrumental in advancing administrative considerations due to her extensive experience in mentoring graduate students in the School of Life Sciences Graduate College. Dr. Gonzales patiently developed my research capabilities from my master's degree at the University of Arizona and has extended her mentorship to my doctoral work. Dr. Liu has helped immensely with technical details of conducting immunology research, guiding the direction of these projects from inception, data analysis and presentation, and the entire process of drafting paper manuscripts to submission and finally approach towards revisions. Dr. Ducruet has provided invaluable clinical insights to for the doctoral works, expanding my scope of my thinking and influencing the work towards increased translational value. I am indebted to Dr. Sattler for helping me navigate administrative issues big and small, her advocacy was crucial. I am also grateful to the SOLS Graduate Office and the SOLS Completion Fellowship.

TABLE OF CONTENTS

Page

LIST OF TABLES……..vi

LIST OF FIGURES……..vii

GLOSSARY OF TERMS…….....x

CHAPTERS

1. INTRODUCTION…….....1
    A. Preface……...1
    B. Clinical Aspects of Intracerebral Hemorrhage, a Severe Form of Stroke……1
    C. Primary and Secondary Brain Injury Following ICH……3
    D. Therapeutic Approaches for ICH……...4
2. BACKGROUND……..……9
    A. Focal Immune Activation Following ICH……..9
    B. Interleukin (IL)-15……...10
    C. Hematopoietic System……13
3. METHODOLOGY
    A. Human Samples……....15
        i. Human Brain Sections……15
        ii. Human Bone Marrow……...15
    B. Mice
        i. ICH Model and Assessment of Neurological Deficit……...16
        ii. Assessment of Brain Edema……..17
        iii. Assessment of Hematoma Volume……...18
    C. Experimental Techniques
        i. ^{18}F-FDG PET Imaging……18
        ii. Flow Cytometry……19
        iii. Drug Treatment……20

CHAPTER Page

iv. Transcriptome Sequencing of Mouse HSCs……21

v. Immunostaining……21

D. Statistical Methods……21

4. INTERLEUKIN-15 BRIDGES ASTROCYTE-MICROGLIA CROSSTALK AND EXACERBATES BRAIN INJURY FOLLOWING INTRACEREBRAL HEMORRHAGE

A. Robust Upregulation of IL-15 in Astrocytes Following ICH in Humans and Mice……..23

B. Astrocyte-targeted Expression of IL-15 Exacerbates Hemorrhagic Brain Injury in Mice……25

C. Astrocyte-targeted Expression of IL-15 Skews Microglia Towards a Proinflammatory Phenotype after ICH……30

D. Microglial Depletion Ablates the Augmentation of Hemorrhagic Injury in GFAP-IL-15^{tg} Mice……33

E. Summary……..34

5. BRAIN INJURY INSTRUCTS BONE MARROW CELLULAR LINEAGE DESTINATION THAT SUPPRESSES NEUROINFLAMMATION

A. ICH Swiftly Activates Bone Marrow Hematopoietic Response in Human…….35

B. ICH Induces Myeloid Bias of Bone Marrow HSCs with Increased Production of Ly6C^{low} Monocytes……38

C. Newly Emergent Ly6C^{low} Monocytes Accumulate in the ICH Brain and Highly Express Anti-inflammatory Factor IL-10……40

D. Increased Sympathetic Tone Induces Bone Marrow Hematopoiesis Response after ICH……..41

E. Upregulation of Small RhoGTPase Cdc42 in Bone Marrow HSCs after ICH…...42

F. Blockade of Cdc42 Abolished ICH-induced Increase of Monocyte

CHAPTER Page

Hematopoiesis in Bone Marrow and Exacerbates ICH Injury…….43

G. β3 agonist Mirabegron Enhances ICH-induced Production of Ly6C^{low} Monocytes and Hematoma Clearance…….46

H. IL-3 treatment accelerates hematoma clearance and functional recovery after ICH……..……..49

I. Summary……..52

6. DISCUSSION

A. IL-15 Bridges the Crosstalk Between Astrocytes and Microglia after ICH……53

B. ICH Induces Anti-inflammatory Ly6C^{low} Monocyte Hemopoiesis That Benefits Stroke Outcome……..56

7. CONCLUSION & FUTURE PERSPECTIVES..……..…….58

REFERENCES……64

LIST OF TABLES

Table		Page
1	Therapeutic Approaches to ICH	9
2	Outstanding Questions in ICH Immunology	64

LIST OF FIGURES

Figure		Page
1	The evolution of Brain Hematoma and PHE in ICH Patients	3
2	Pathological Events Following ICH	8
3	Hematopoiesis of Monocytes and Their Fate	15
4	Upregulation of Astrocytic IL-15 after ICH in Humans and Mice	26
5	Astrocyte-targeted Expression of IL-15 in GFAP-IL-15^{tg} Mice	28
6	Astrocyte-targeted Expression of IL-15 Exacerbates Hemorrhagic Brain Injury	28
7	Effects of Astrocyte-targeted Expression of IL-15 on Hemorrhagic Brain Injury in Autologous Blood Injection Model	29
8	Effects of Astrocyte-targeted Expression of IL-15 on Brain Edema after ICH	30
9	Effects of IL-15 Neutralization or Knockdown of Astrocytic IL-15 on ICH Injury in WT Mice	31
10	Augmented Microglia Response in GFAP-IL-15^{tg} Mice after ICH	33
11	Skewed Microglia Response Toward a Proinflammatory Phenotype in GFAP-IL-15^{tg} Mice after ICH	34
12	Depletion of Microglia Diminishes the Exacerbation of ICH Injury in GFAP-IL-15^{tg} Mice	35
13	ICH Induces a Swift Response in Bone Marrow of ICH Patients	38
14	ICH Increases Bone Marrow Uptake of ^{18}F-FDG	39
15	ICH Increases Bone Marrow HSC Activity	39
16	Lineage Tracing of Genetically Labeled HSCs and Their Fate in ICH Mice	41
17	Newly Emerged Ly6C^{low} Monocytes Transmigrate to The Brain of ICH Mice	42
18	Blockade of Adrenergic β3 Receptor Diminished ICH-induced Increase of HSC Activity in Bone Marrow	43
19	ICH Induces a Profound Transcriptome Change of HSCs	45

Figure		Page
20	Cdc42 Inhibition Abolishes ICH-induced Increase of Monocyte Hematopoiesis in Bone Marrow	46
21	Cdc42 Inhibition Reduces Ly6^{low} Monocytes in the ICH Brain and Exacerbates ICH Injury	47
22	An Adrenergic β3 Receptor Agonist Enhances Bone Marrow Production of IL-10-Producing Ly6C^{low} Monocytes after ICH	49
23	Adrenergic β3 Receptor Activation Reduces Brain Inflammation and Improved Hematoma Clearance	50
24	IL-3 Treatment Enhanced ICH-induces Hematopoiesis of Ly6C^{low} Monocytes in the Bone Marrow	52
25	IL-3 Treatment Reduces Brain Inflammation and Promoted Hematoma Clearance after ICH	52
26	IL-15 Bridges Astrocyte-microglia Crosstalk and Exacerbates Brain Injury Following ICH	55
27	ICH Induces Bone Marrow Hematopoiesis of Ly6C^{low} Monocytes That Reduce Brain Inflammation and Accelerate Hematoma Clearance	58
28	Peripheral and CNS Approaches to Control ICH-triggered Neuroinflammation and Neurodegeneration	63

GLOSSARY OF TERMS

BBB	Blood brain barrier
CNS	Central nervous system
CSF1R	Colony stimulating factor 1 receptor
CMP	Common myeloid progenitor
CLP	Common lymphoid progenitor
DWI	Diffusion weighted imaging
DAMP	Damage-associated molecular patterns
GFAP	Glial fibrillary acidic protein
GMP	Granulocyte-monocyte progenitor
HSC	Hematopoietic stem cell
ICH	Intracerebral hemorrhage
MRI	Magnetic resonance imaging
MDP	Monocyte-dendritic cell progenitor
mNSS	Modified neurological severity score
MMPs	Matrix metalloproteinases
PET	Positron emission tomography
PHE	Perihematomal edema
PFA	Paraformaldehyde
PPARγ	Peroxisome proliferator activated receptor-gamma
SNS	Sympathetic nervous system
S1PR	Sphingosine-1-phosphate receptor

CHAPTER 1

INTRODUCTION

Preface

Acute central nervous system (CNS) injuries, including brain ischemia, intracerebral hemorrhage (ICH), and traumatic brain injury, swiftly trigger immune responses within and outside the brain[1-3], profoundly impacting the brain as well as peripheral organ systems[4-7]. A comprehensive understanding of the focal and systemic effects of brain injury on the immune system is therefore critical for an elucidation of the pathophysiology of these acute disorders to identify new therapeutic strategies to improve disease outcomes. To address these questions, the ultimate goal of my study was to characterize the impact of acute brain insults, in the context of ICH, on focal and systemic immune responses as well as their influences on neurological outcome.

Clinical aspects of intracerebral hemorrhage, a severe form of stroke

The World Health Organization defines stroke as “rapidly developing clinical signs of focal, at times global, disturbance of cerebral function, lasting more than twenty-four hours or causing death with no apparent provenance other than of vascular origin.” The carotid and vertebral arteries are the entry point for the vascular supply to the brain and branch in the brain perfusing corresponding regions. The adult brain requires 20% of the body’s oxygen consumption to continuously supply glucose and oxygen. Deprivation of either substance as caused by stroke results in neuronal death and dysfunction within minutes. Stroke continues to be a major public health problem, ranking in the top five causes of death in developed countries and represents a large proportion of the burden of neurologic disorders.

Stroke is categorized by the pathology of the focal brain injury as being either infarction or hemorrhage. Intracranial hemorrhage is the pathological accumulation of blood within the cranial vault which may occur within brain parenchyma or the surrounding meningeal spaces as a result of the rupture of a vessel within the cranium. In all, intracranial hemorrhage accounts for 10-15%

of all strokes, however, incidence varies depending on variables such as country of origin and ethnicity. Here, intracerebral hemorrhage (ICH) refers, specifically, to spontaneous intra-parenchymal bleeding.

A wide spectrum of causes from hypertensive changes or vascular abnormalities may lead to the rupture of brain blood vessels leading to ICH. The most common cause of the rupture of cerebral penetrating arteries is hypertension, which has been implicated as a cause of deteriorating integrity of the arteriole walls, such as Charcot-Bouchard aneurysms. Arterial blood ruptures under pressure and destroys or displaces brain tissue. These arterial hemorrhages are typically located in the basal ganglia, thalamus, pons, cerebellum, or deep white matter. The extravasation of blood into the parenchyma forms a hematoma which may disrupt and compress adjacent brain tissues, causing neuronal dysfunction and death. Moreover, it is recently recognized that bleeding may continue for several hours following ictus and the hematoma may expand. Hematoma formation and expansion is accompanied by an increase in intracranial pressure and edema which further damage tissue and may cause herniation. Herniation, midbrain or pontine hemorrhage, intraventricular hemorrhage, acute hydrocephalus, and/or dissection into the brain stem can impair consciousness causing coma or death.

Varying prognoses are dependent upon the hemorrhage location, size, and cause of bleeding, ICH is more likely to result in death or major disability than ischemic stroke[8, 9]. Case fatalities are worse for hemorrhagic strokes, ranging from 30-80%. The first-year mortality of ICH is about 50%, over 70% in 5 years, and only 20% patients live independently after 6 months[10, 11]. Survival is influenced by age, hypertension, cardiac disease, and diabetes. The neurologic symptoms of ICH are dictated by the location and size of the hematoma. General symptoms are characterized by headache, vomiting, and the dynamic development of focal or sensory manifestations from minutes to hours after the stroke. Consciousness is another prominent symptom and may be impaired with moderate and large hematomas in the first 24-48 hours.

Intraparenchymal hemorrhage is commonly identified as a signal density on head CT and/or as a signal of varying intensity on MRI.

Primary and secondary brain injury following ICH

ICH has both primary and secondary injury components followed by a period of repair. The elements and effects of primary injury are mostly non-modifiable. Primary brain injury induced directly or indirectly by hematoma includes significant death of brain cells, including necrosis, apoptosis, and autophagy around the clot. The inflammatory cascade that accompanies ICH accelerates formation of edema around the hematoma, defined as peri-hematomal edema (PHE). The dynamic of PHE relative to hematoma can be visualized in ICH patients by CT (**Figure 1**). PHE exacerbates cell death and brain tissue damage[1, 3, 12], which induces a severe secondary injury and the destruction of adjacent tissue, in addition to impairing the integrity of the blood-brain-barrier (BBB). The immune response, triggered mere minutes following ICH, evolves to peak just days thereafter and may persist for weeks to months after ictus, serving as biological basis for PHE. ICH activates the immune system that involves inflammatory response within the brain and peripheral immune alterations following disease onset. Cell death products such damage-associated molecular patterns (DAMP) activate microglia, which coordinate a cascade of events leading to inflammation. ICH also mobilizes peripheral neutrophils, monocytes, natural killer (NK) cells, T cells and B cells, that transmigrate into the brain.

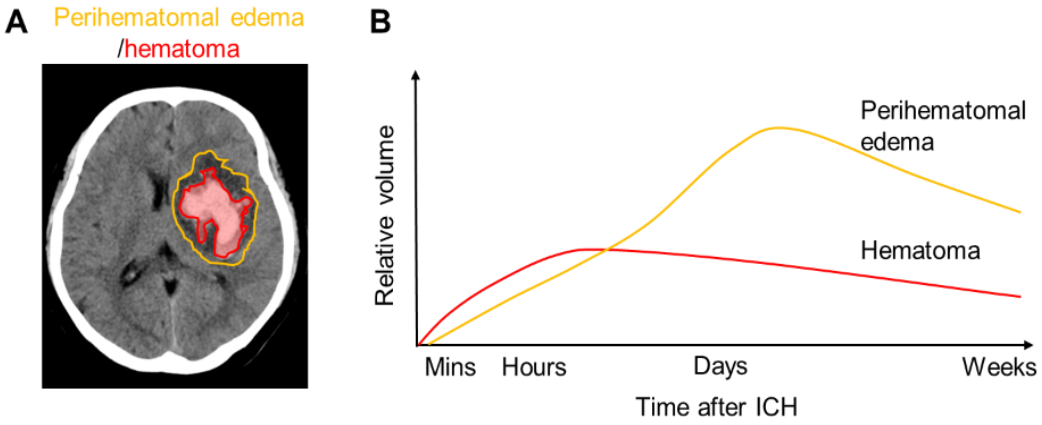

Figure 1. Evolution of brain hematoma and PHE in ICH patients. (A) A CT image showing PHE and hematoma region in the brain of an ICH patient at 24 hours after onset. (B) Schematic diagram of the evolution of PHE and hematoma in ICH patients.

Therapeutic approaches for ICH

ICH is primarily a spontaneous occurrence. This sudden onset complicates the clinical approach to management and along with its high attendant rates of mortality and permanent disability makes the condition a medical emergency[1, 8, 13]. There are urgent unmet needs for effective therapies to improve the outcomes for ICH, as current management of ICH is limited to supportive care. The general principles for the care of ICH patients is restricted to the major issues of: preventions of continued hemorrhage by early correction of coagulation and platelet abnormalities; early control of elevated blood pressure; identification and control of urgent surgical issues such as mass effect, intracranial hypertension, and hydrocephalus; definitive diagnosis of cause of hemorrhage and treatment of underlying cause. Although no specific therapies improve the outcome after ICH, recent progress in the understanding of the complex mechanisms involved in ICH-induced injury presents new targets for novel intervention.

The therapeutic time window for modulating brain repair may be longer than for preventing ICH-induced brain injury. Mass effect and mechanical disruption from the initial hemorrhage causes primary brain injury. This initial physical distortion of brain cells and their connections by

the hemorrhage kills the cells in the immediate vicinity and are beyond rescue, limiting further tissue damage and rescue of damaged brain cells guide the objectives for experimental interventions.

The pragmatic clinical question of the efficacy of clot removal remains outstanding. Results from recent trials of minimally-invasive hematoma evacuation and the use of iron chelators did not demonstrate effectiveness[44-46]. In particular, CLEAR III was performed on a small and selective sample of patients with intracerebral bleeding and obstructive hydrocephalus from intraventricular hemorrhage at the end of the current treatment spectrum. CLEAR III trial shows that clot removal in intraventricular hemorrhage is neutral on functional outcome; secondary analyses suggests that clot removal may improve mortality at the cost of increased disability, nevertheless, trial authors suggest that current practices should not change[53] (**Table 1**).

A cardinal element affecting ICH outcome is hematoma size and hematoma expansion. The expansion of the hematoma is a common occurrence in the pathology of ICH, enlargement of the hematoma is reported in nearly a third of ICH patients in the first 24 hours after ictus[14]. Preliminary histopathological studies provide evidence that the presence of microscopic and macroscopic bleeds in the area surrounding hematoma may represent ruptured arterioles or venules[15, 16]. More recent studies based on CT and SPECT techniques have shown that in some patients, early hematoma growth is associated with secondary bleeding in the periphery of the existing hematoma and into congested areas of the perihematomal tissue[16, 17]. Risk factors identified for hematoma expansion include blood pressure, vascular, and hematological disorders. Hematoma growth enhances both primary and secondary injury by compounding brain tissue damage, prolonging bleeding, and contributing to the formation of edema. Consequently, much attention is centered on modifying hematoma evolution through a variety of approaches ranging from anti-hypertensive to hemostatic therapies. Several clinical trials have investigated the prospect of blood pressure control for ICH, yet such approaches have either failed to reduce hematoma expansion or meaningfully improve outcomes[18]. Clinical trials establishing early

hemostasis to stem hematoma growth have similarly reported inconclusive results; trials with Factor VIIa, a thrombotic drug approved for patients with hemophilia, report reduction in hematoma volume but neither improved survival or functional outcome following ICH in the latest phase III trial (NCT03496883)[19, 20].

PHE has also been implicated as a contributing factor for delayed neurologic deterioration after ICH[21]. Secondary injury manifested by PHE occurs over an extended period from hours to weeks thereafter[3]. Edema formation after ICH progresses through characteristic several phases: the hyperacute phase involves trans-endothelial osmotic pressure, clot retraction, and cytotoxic edema in the first several hours; the acute phase elapsing in the first day is characterized by the clotting cascade, thrombin production, and inflammatory activation; and the third phase, beginning approximately 72 hours post-ICH, is marked by erythrocyte lysis and hemoglobin-induced neurotoxicity[16, 22, 23]. PHE is the result of both BBB disruption and local generation of osmotically active substances that spread to adjacent structures[16]. In ICH, PHE causes progressive tissue injury and the extent of PHE directly correlates with adverse outcomes[3, 24-26]. The close association with clinical outcome and extended functional timeframe qualifies the management of edema as an attractive therapeutic approach to treat ICH (**Figure 2**)[2, 27-30].

Mannitol is an intravascular osmotic agent often used in clinic to control brain edema resulting from trauma or stroke. Although guidelines recommend using mannitol where there is increased intracranial pressure in ICH, the effects of mannitol in large clinical trials of ICH patients fail to produce definitive evidence of benefits[31, 32]. Preclinical and retrospective clinical data indicate that glyburide, a small molecule channel blocker, is effective in preventing edema and improving outcome after focal ischemia[33]. Various preclinical studies demonstrate glyburides effect in attenuating brain edema and outcome in ICH; however, most large clinical trials of glyburide are conducted in the context of ischemic stroke, tolerability and efficacy in ICH is undetermined.

Other strategies target processes driving acute PHE formation, which are broadly encompassed by three intertwined neurotoxic cascades: inflammation, erythrocyte lysis, and thrombin production. Fingolimod is an oral drug approved to control disease activity in multiple sclerosis; it is a sphingosine-1-phosphate receptor (S1PR) modulator which inhibits the egress of lymphocytes from secondary lymphoid organs to the brain. A pilot trial in ICH patients shows fingolimod, administrated within 72 hours after hemorrhage, inhibited PHE expansion and improved clinical outcome[34]. Based on these results, a phase 2 trial using a secondary S1PR1 selective modulator, BAF312, has been initiated in North America and the results are awaiting (NCT03338998). Hemolytic breakdown of erythrocyte components of the hematoma occurs from days to weeks after the sentinel hemorrhage event, is another component process targeted in attenuating PHE expansion and secondary injury. Intact erythrocytes undergo lysis and release cytotoxic products hemoglobin, heme, and iron, which create a highly oxidative and cytotoxic environment that triggers secondary processes which negatively influence the viability of brain cells surrounding the hematoma[8, 35-37]. Thus, the timely removal of erythrocytes may limit the toxic effects of persistent blood components on surrounding tissue and improve ICH recovery. The inconclusive trial resulting from surgical clot retraction interventions has shifted the emphasis towards amplifying endogenous mechanisms of hematoma resolution. Preclinical studies demonstrate that modulation of peroxisome proliferator activated receptor-gamma (PPARγ) with pioglitazone expedites hematoma resolution by enhancing monocyte/macrophage phagocytosis in the rodent ICH model; however, the exact protective mechanism is not definitive due to pleotropic nature of the PPARγ agonist used [38]. Nevertheless, preclinical pioglitazone results galvanized the Safety of Pioglitazone for Hematoma Resolution in Intracerebral Hemorrhage (SHRINC; NCT00827892) clinical trial examining drug efficacy on hematoma and edema resolution in ICH patients, study results have not been publicly reported since completion[39].

Here, I highlight the notable preclinical and clinical studies which aim to improve outcomes in ICH by modulating the many factors involved in worsening hemorrhagic brain injury. Extensive basic and clinical research towards the understanding of the pathophysiology of the disease have

established a starting point for treatment strategies in the identification of modifiable targets. Treatment strategies have broadly targeted; reducing hematoma expansion, promoting endogenous hematoma clearance or clot evacuation, and management of PHE formation and development (**Figure 2**). Although each approach represents a viable direction for the development of an intervention, an effective treatment for ICH has yet to be discovered. Indeed, insights to the disease may be interrogated not only from the reported results from ongoing and completed clinical trials, but also in overall trial aims and designs. The majority of the pharmacotherapeutic trials reviewed naturally targets a singular aspect, whether a receptor or mechanistic event, of many driving secondary injury. Secondary injury in ICH is characterized by its interactive and multi-dimensional nature; the manifold signaling pathways and molecular mechanisms which govern the discrete responses initiated in response to primary injury, like inflammation and PHE, converge and integrate to advance brain injury (**Figure 2**). Thus, pharmacological intervention strategies that modulate key signaling or molecular factors implicated secondary injury may be compensated by redundant pathways or simply eclipsed by the higher components within secondary injury. Moreover, many other factors such as focal and systemic inflammation, coagulation and thrombin responses, glial cell interaction and crosstalk, are among the many other considerations which may affect and complicate efficacy of experimental interaction; and may explain why surgical intervention trial results where clot evacuation diminished PHE in some ICH patients but did not achieve functional improvement. A comprehensive understanding of ICH pathology is still unclear. Major questions around the focal response and especially the systemic aspects of the disease require further clarification. Thus, the major aims of my work seek to advance the field by filling existing knowledge gaps of focal and systemic immune responses to ICH.

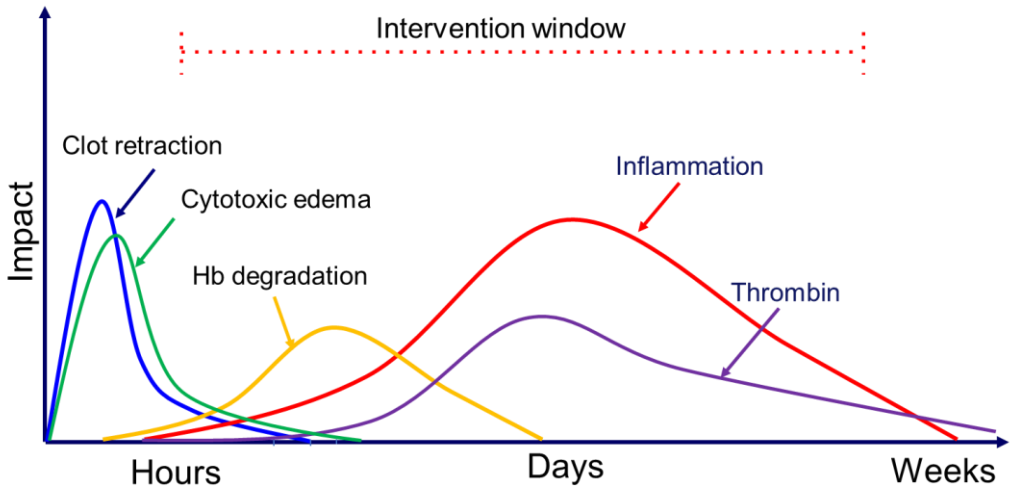

Figure 2. Pathological events following ICH.

Table 1. Therapeutic Approaches for ICH.

Targeting hematoma	**Findings**
Surgical removal	No benefit on mortality and prognosis[47-49]
MISTIE (mini-invasive surgery + tPA)	Safely cleared hematoma; probably improve outcome and additional study needed; increase asymptomatic hemorrhage[44, 50, 51]
Deferoxamine	Safe for ICH patients; primary endpoint was not met[13]
Targeting edema	
Mannitol/glycerol fructose	No evidence of benefit[31, 32]
Glyburide	Preclinical results suggest reduction of brain edema[33]
BAF312 (S1P1/S1P5 modulator)	Phase II, ongoing (NCT03338998)

CHAPTER 2

BACKGROUND

Focal immune activation following ICH

Despite the continuous attempts at hematoma removal and prevention of hematoma expansion, presently, effective therapeutic interventions for ICH patients are still lacking[3, 55, 56]. Release of DAMPs by injured neural cells and hematoma components quickly activates the immune responses within the brain after ICH. In the early stages of ICH, the infiltration of hematogenous immune cells into the injured brain begins within hours after ICH. Among immune cell subsets, myeloid cells such as neutrophils and monocytes arrive to the ICH brain early after onset and produce proinflammatory factors such as tumor necrosis factor-α (TNF-α), interleukin (IL)-1β, matrix metalloproteinases (MMPs), which augments focal inflammation and BBB disruption, leading to exacerbated brain damage. Besides myeloid cells, lymphocytes appear in the cerebrospinal fluid as early as 6 hours after ICH, and are further detected in the perihematomal brain tissue of ICH patients[27, 57]. In animal models of ICH, brain infiltration of multiple lymphocyte

subsets such as $CD4^+$ T, $CD8^+$ T, B, and natural killer (NK) cells are observed within 24 hours after ICH, peaking around day 3 after ICH. During the late stage of ICH, phagocytic cells are mobilized to clear extravagated erythrocytes in the hemorrhagic brain to offset the cytotoxic effects of blood components. Microglia and macrophages are professional phagocytes that engulf cellular debris at tissue injury site. Although these findings suggest a contribution of macrophages in hematoma resolution, the role of other immune cell subsets in ICH recovery remains poorly understood.

Emerging evidence has demonstrated that the inflammatory cascade accelerates the formation of PHE post-ICH, exacerbating the mass effect and worsening neurological outcome[8, 27, 30, 58]. Microglia are among the very first responders of injury, detecting danger signals via their expression of pattern recognition receptors. Upon activation, microglia engages in intimate crosstalk with other brain cell types and infiltrating leukocytes that enter the brain from the periphery through the compromised BBB[8, 59]. Following ICH, microglia display features of phagocytosis, antigen presentation, and production of inflammatory mediators including IL-1β and TNF-α[30, 59]. In addition, microglia also possess anti-inflammatory properties by releasing factors such as IL-4 and transforming growth factor-β (TGF-β), and facilitate inflammation resolution and repair processes of brain injury[59, 60]. These features imply an active participation of microglia in the evolution of secondary injury and tissue repair in ICH. However, the focal signals within the injured brain that control the activity of microglia following ICH remain unclear. While astrocytes are the predominant glial cell population within the brain, the molecular mechanisms by which astrocytes initiate and instruct microglia response also remains unknown.

Interleukin (IL)-15

IL-15 is a pleiotropic cytokine with a broad range of biological functions in many diverse cell types. IL-15 is mainly membrane bound, and it induces signaling via cell-cell contact. IL-15 is constituted by a 4 α-helix bundle, a member of the common gamma-chain cytokine family. The conserved molecular structure of IL-15 and IL-2 consequently share two common receptor

subunits, with the α-subunits distinguishing their respective heterotrimeric receptors. Its receptor is expressed by hematopoietic cells, particularly T cells and NK cells, the unique subunit of the IL-15R, IL-15Rα, presents IL-15 *in trans* to neighboring cells mediating signal transduction through the common Janus kinase (JAK) and signal transducer and activator of transcription (STAT) signaling molecules[61, 62].

IL-15 regulates the magnitude and intensity of immune responses, thus has both normal protective functions but also pathological implications. The diverse role of IL-15 in adaptive immunity is well reported; IL-15 activates T cells and NK and enhances their cytolytic responses[61, 63], it is also pivotal in the maintenance of long-lasting, high-avidity $CD8^+$ memory T cells. Peripherally, IL-15 is known to contribute to the immune pathology of several inflammatory diseases such as rheumatoid arthritis and inflammatory bowel disease[64, 65]. Within the CNS, astrocytes are a major source of IL-15 after injuries[66, 67]. Although previous studies demonstrate the divergent effects of IL-15 in exacerbating or attenuating inflammation and neural injuries depending on the timing and disease types[66-70], to what extent and by which mechanisms IL-15 influences neuroinflammation and brain injury in the setting of ICH is presently unknown.

In ICH patients and a murine model of ICH, we found that IL-15 is dramatically upregulated in astrocytes. To understand the potential role of astrocyte-derived factors such as IL-15 in ICH, we generated a transgenic mouse line with targeted expression of IL-15 in astrocytes (GFAP-IL-15^{tg}) and examined ICH injury in these mice. In the first part of this study, I investigated the crosstalk between astrocyte and microglia in the acute phase of ICH that involved IL-15. Our findings demonstrate that IL-15 is a key factor of astrocytes which increases microglia activity and exacerbates brain injury following ICH.

The impact of ICH on immune system outside the brain: the current understanding

The nervous system and immune system interact with each other at multiple points and levels in a well-balanced equilibrium at stasis. Brain injuries often interrupt such balance and induces

profound alterations to the body. Brain injuries such as ICH not only triggers focal immune responses within the brain but also induce systemic immune alterations that are critical to the disease outcome. Studies have suggested that brain injuries induced profound systemic changes in organs such as the spleen[4], heart[71], intestine[72], liver[73], etc. The response of these organ systems have critical impacts on the disease outcome[4, 72, 73]. For instance, during the acute stage, ischemic stroke-induced spleen atrophy and lymphopenia severely harm the immune defense functions of patients which is associated with increased infectious complications[4, 5]. The heart is also reported to undergo functional and structural changes after stroke, which may potentially have long-lasting impacts on cardiovascular system[71, 74, 75]. The microbiota-induced immune response within the intestinal wall post-stroke is associated with brain inflammation and stroke outcome[72, 76]. In ICH, injury induced significant spleen atrophy as well as lymphocyte deficiency during the acute phase in both patients and animal models. The immunosuppression after ICH is associated with increased infections and worsened clinical outcome[4].

Different from lymphocytes, circulating monocytes populations display an increasing trend after ICH[4]. Following ICH, peripheral monocytes are rapidly recruited to the brain and quickly outnumber other infiltrating leukocyte subsets[57, 77, 78]. Upon entry to the brain, monocytes differentiate into macrophages, which have been reported to be temporally and spatially associated with hematoma clearance[58, 79, 80]. Although these findings suggest the contribution of macrophages in hematoma resolution, the role of monocytes and their descendent macrophages are not universally beneficial in ICH.

Peripheral blood monocytes are defined by their expression of the cell surface markers; lymphocyte antigen 6 complex, locus C1 (Ly6C) is a 14 KD differentiation antigen, expressed on macrophage/dendritic cell precursors in mid-stage development (late CFUM, monoblasts, and immature monocytes), granulocytes, and on a wide range of endothelial cells and subpopulations of B and T lymphocytes. Ly6C is ideally suited for the detection of monocytes in bone marrow samples by FACS, and it further marks activated macrophages in inflammatory tissues.

Reportedly, amongst brain-infiltrating monocytes, the Ly6C^{high} subset of monocytes and their descendent macrophages are acute responders to inflammation and disseminate pro-inflammatory factors which augment secondary injury[36, 78]. In contrast, the Ly6C^{low} subset of monocytes and their derivative macrophages produce anti-inflammatory factors and accelerate erythrocyte phagocytosis, leading to improved ICH recovery[58, 80, 81]. Together, these findings implicate macrophages as major contributors towards hematoma resolution following ICH and indicate that enhancement of Ly6C^{low} monocytes and their descendent macrophages could be harnessed as a viable approach to accelerate hematoma resolution and improve ICH outcomes.

Hematopoietic system

The hematopoietic system harbors the enormous capability of cell proliferation and differentiation to meet the demands of blood and immune cell production during periods of homeostasis and stress[82-85]. All blood cells are derived from hematopoietic stem cells (HSCs), which predominantly reside in the bone marrow niche, and are capable of self-renewal and differentiation into various immune cell types, including myeloid cells. Amongst the differentiated progeny of HSCs, monocytes have a short life span of hours to a few days and thus have a limited population in blood[86-88]. Several prior studies have suggested that monocytes and their macrophage descendants may impact ICH outcome[57, 77, 78]. Following ICH, myeloid cell reservoirs in the marginal blood pool, the bone marrow, and the spleen are rapidly exhausted[89-91] (**Figure 3**). To offset the neurotoxic effects of erythrocyte hemolysis, phagocytic cells are mobilized to clear extravasated erythrocytes in the hemorrhagic brain[35, 79, 92, 93]. Macrophages in particular are professional phagocytes that engulf cellular debris at tissue injury site, peripheral monocytes are rapidly recruited to the brain and their derivative macrophages outnumber other infiltrating leukocyte subsets in the parenchyma[57, 77, 78]. The short life span of circulating monocytes and

their tissue resident macrophage are rapidly depleted and thus need replenishment from hematopoiesis system to maintain a sufficient supply.

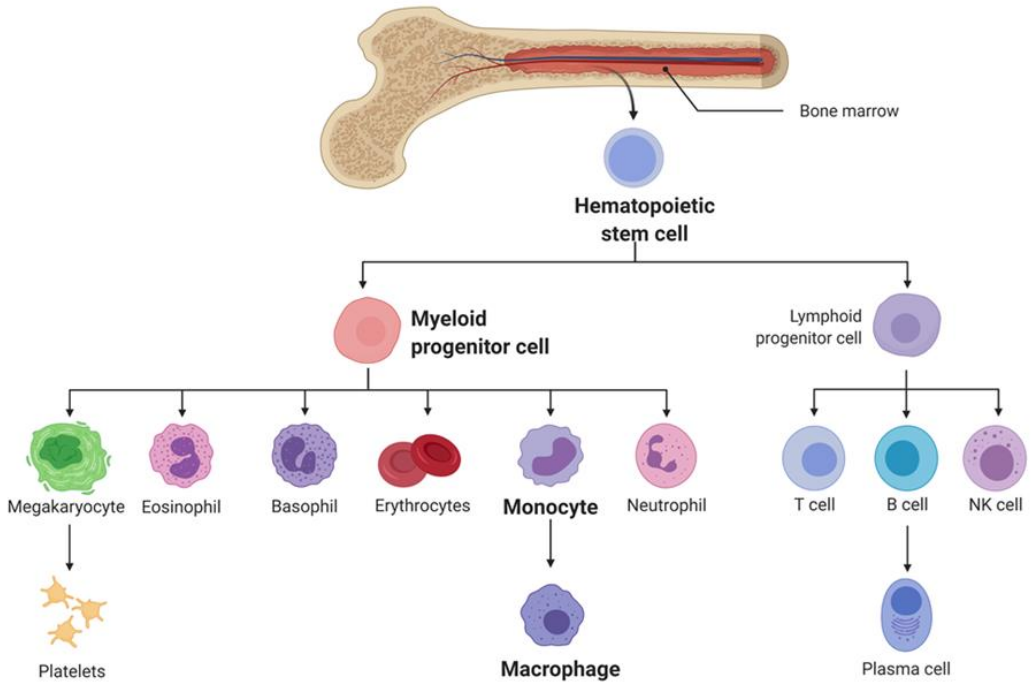

Figure 3. Hematopoiesis of monocytes and their fate.

ICH activates adrenergic innervation that induces lymphocyte hypo-function and causes lymphopenia[4, 94]. In contrast to the reduced numbers of blood lymphocytes, the surge of circulating monocytes post-ICH implies the involvement of a continuous supply of monocytes originating from the bone marrow. In this regard, several key questions remain unanswered. First, because bone marrow is the primary site for adult hematopoiesis, as an immune organ what is the precise influence of ICH on bone marrow hematopoietic cells? Second, what are the long-range signals that mediates the communication between the injured brain and bone marrow? Third, hematopoiesis is tightly regulated by intracellular machinery of hematopoietic stem cells (HSCs) to provide a balanced output of different leukocyte subtypes, what is the key molecular switch that control the HSC response to ICH? Fourth, what is the fate of the newly produced immune cells, specifically the monocytes derived from bone marrow? Lastly, what is the impact of

newly generated monocytes on neuroinflammation and neural injury in ICH? These major questions underlie the rationale for understanding how the hematopoietic response to ICH. Therefore, I investigated the neurogenic pathways governing monocyte hematopoiesis and their potential contribution to ICH injury and hematoma resolution.

CHAPTER 3

METHODOLOGY

Clinical Samples

Human brain sections

Paraffin-embedded brain tissue sections were obtained from the Banner Sun Health Research Institute (Sun City, AZ). Among the 12 brains studied, 6 (4 male, 2 female) were from patients who died from ICH. The other 6 (4 male, 2 female) were from individuals without past history of neurological, psychological, or systemic inflammatory diseases. These were used as controls. ICH patients and control subjects did not differ significantly for mean age at death (ICH vs. Control: 86 ± 7 vs. 88 ± 5 years, Mean ± SEM, $P = 0.46$, two-tailed unpaired Student's *t* test). Brain tissues were collected within 4 hours after death.

Human bone marrow

Bone marrow samples were obtained from cranial bone flaps removed from ICH patients undergoing decompressive surgery. Cranial bone segments were flushed with ice cold PBS into a conical tube and subsequently kept on ice and samples were processed immediately after intake. Patients with unruptured aneurysm undergoing surgery clipping were recruited as controls. Patients or their surrogate gave consent before sample processing. Bone marrow from 6 ICH patients and 13 controls were collected for this study; among these, 3 ICH samples and 8 control samples were excluded due to poor sample quality. Therefore, 3 ICH (2 female, 1 male, 64 ± 6 years) and 5 controls (4 female, 1 male, 69 ± 10 years) are included for data analysis. The average time from disease onset to operation of ICH patients is 22 ± 11 hours.

Animal Model

Mice

Male C57BL/6 (B6) mice were purchased from Taconic (Taconic Biosciences). GFAP–IL-15^{tg} mice were generated by using a GFAP-promoter to direct astrocyte-specific transcription[93]. Fgd5-CreER-tdTomato mice were obtained by crossing Fgd5-CreERT2 mice with B6.Cg-Gt(ROSA)26S mice (both lines were purchased from Jackson Lab). Fgd5 has shown to be specifically expressed in HSCs and the Fgd5-CreER allele exhibits tamoxifen-inducible CreER activity exclusively in long-term HSCs, and their downstream cell lineages will consistently express tdTomato[92]. All transgenic mouse lines were back-crossed to the B6 background for 12 generations. For all experiments, 8- to 12-week-old, 23–25 g body weight, age-matched littermates were used. All mice were randomly assigned to experimental groups. Randomization was based on the random number generator function in Microsoft Excel 2016. Mice were housed under standardized light-dark cycle conditions with access to food and water ad libitum. All surgeries were performed under ketamine/xylazine anesthesia. Mice were housed in pathogen-free conditions at the animal facilities. All animal experiments were performed in accordance with the recommendations of the Guide for the Care and Use of Laboratory Animals of the National Institutes of Health and in accordance with the ARRIVE (Animal Research: Reporting *In Vivo* Experiments) guidelines. Animal studies were approved by the institutional Animal Care and Use Committees.

Collagenase injection ICH model and assessment of neurological deficit

ICH was induced by stereotactic injection of collagenase IV (ThermoFisher) to the basal ganglia region of mice brain as described[4, 95]. Briefly, surgeries were conducted in a sterile manner, following induction of surgical plane anesthesia via intraperitoneally injection of ketamine/xylazine mix, hair at the top of the cranium was shorn and disinfected with 70% ethanol. Mice were

positioned in the stereotactic instrument and superficial incision at the cranium was made. From the bregma, 2.3 mm right and 0.5 mm forward, a small craniotomy of 1 mm burr hole was made with special attention to avoid perforation of the dura by the drill bit. The Hamilton syringe with a 30g needle was then inserted 3.7 mm down into the striatum, controlled injection of 0.03 U of collagenase was administered via micro-injection pump. Upon injection completion, needle was left in for 5 min to prevent backflow, and subsequently withdrawn. Incision was then sutured with 5-0 Ethicon silk sutures. The neurological deficits of mice were evaluated by modified neurological scale score (mNSS) as we described previously[95, 96]. mNSS comprehensively evaluate the motor, sensory, reflex, and balance functions by a battery of tests. In addition, the sensorimotor function of mice were evaluated by Cylinder test as described[95, 97], in brief, mice were placed in a clear glass cylinder and were allowed to rear for 20 times in total, the first forelimb touch the cylinder wall during rearing was recorded. A laterality index was calculated by [(right-left)/(right+left+both)]. The higher laterality indicates a more severe left hemiparesis.

Assessment of brain edema

PHE volume of ICH mice was quantified on images acquired by a 7-Testa small animal magnet resonance imaging (MRI) scanner (Bruker, Billerica, MA) as previously described[5, 96, 98]. Mice were under anesthesia by inhalation of 3.5% isoflurane and maintained by inhalation of 1.0–2.0% isoflurane in 70% N_2O and 30% O_2 via nose cone. Throughout MRI scan, the animal's respiration was continually monitored by a small animal monitoring and gating system (SA Instruments, Stoney Brook, NY) via a pillow sensor positioned underneath the abdomen. Mice were placed on a heated circulating water blanket to maintain their normal body temperature (36–37 °C). T2-weighted images of the brain were acquired with fat-suppressed rapid acquisition with relaxation enhancement (RARE) sequence (repetition time, 4000 ms, echo time, 60 ms, slice thickness, 0.5 mm) to measure the lesion volume. Susceptibility-weighted images (SWI, repetition time, 21.0 ms; echo time, 8.0 ms; 0.3-mm thickness) were scanned to measure hematoma volume. Diffusion weighted images (repetition time, 2500 ms; echo time, 27; 1 mm thickness) were

acquired to measure cytotoxic edema[99]. Lesion volume on T2 images and hematoma volume were measured via image J (National Institutes of Health), PHE was calculated by lesion volume minus hematoma volume.

Brain water content was assessed at day 3 after sham or ICH surgery as previously described[98, 100]. Briefly, brains of mice were dissected without perfusion, the wet weight of contralateral hemisphere, ipsilateral hemisphere, and cerebellum were weighted separately. The separated brain tissue parts were then dried at 100°C for 24 hours, after which, the dry weigh of each parts was weighed again. Brain water content was calculated as the percentage of lost weight of each part from wet to dry.

Assessment of hematoma volume

Hematoma volume was detected at day 7 after ICH as described[80]. In brief, mice were sacrificed by inhalation of overdose isoflurane, after perfusion, brains were dissected and fixed in 4% PFA overnight. Thereafter, brains were cut into 2 mm thick sections and high-resolution pictures were captured. Hematoma sizes were calculated via ImageJ, binary images were generated in which hematoma appearing black and brain tissue appearing white. Total hematoma volume was calculated by multiplying the hematoma area with slice thickness.

Experimental Techniques

^{18}F-FDG PET imaging

The bone marrow cell activity was detected by Positron Emission Tomography (PET) imaging of ^{18}F-FDG uptake *in vivo*[101]. At day 3 after ICH induction, mice received an intravenous injection of 100μCi ^{18}F-FDG 1 h before scanning. Mice were then scanned by using a MicroPET small animal scanner (Bruker, Billerica, MA, USA), images were acquired on a field of view of 80cm x 80cm (160 x 160 pixel), and then reconstructed to a three-dimensional projection (336 x 160 x160 pixel). T2-weighted images of each animal were previously acquired by a 7-T MRI scanner (Bruker) to delineate the regions of interest. PET and T2 images were fused to localize the

vertebral bone marrow and data were calculated as mean standard uptake value (SUV). Mice were anesthetized by inhalation of 3.5% isoflurane and maintained by inhalation of 1.0% to 2.0% isoflurane in 70% N_2O and 30% O_2 during all scanning.

Flow Cytometry

Human bone marrow cells were isolated by centrifuging in Ficoll (Sigma-Aldrich, St. Louis, MO, USA) to remove red blood cells and bone debris. Cells were then stained with live/dead staining dye and fluorochrome-conjugated antibodies to evaluate HSC and the lineage progenitors. In mice, brain tissue was finely cut into small pieces and incubated with papain and DNase at 37°C for 30 min for dissociation. After removing the myelin debris by centrifuge in 30% Percoll at 300g for 40min, single cells were then suspended in 1% BSA for antibody staining. Spleen was minced and forced through a 70-μm cell strainer; red blood cells were lysed in lysing buffer. Single spleen cells were suspended in 1% BSA. Bone marrow were collected from femur bones by flushing bone cavity with PBS, single cell suspension was obtained after lysing red blood cells. Single cell suspensions of aforementioned tissues were placed to flow tubes with 10^6 cells per tube and stained with flow cytometry antibodies. Antibodies used in the study are AF647 anti CD3, PE-Cy7 anti CD4, APC-Cy7 anti CD8, BV785 anti CD19, APC-R700 anti CD45, BV510 anti CD11b, APC anti Ly6G, PE anti CD86, BV421 anti TGF-β, Percp anti IL-6, PE-dazzle594 anti TNFα, PE anti IL-1β, BV605 anti IL-4, AF700 anti GFAP, FITC anti NeuN, APC anti IL-15. BV421 anti Lineage (17A2/RB6-8C5/RA3-6B2/Ter-119/M1/70, 133311, Biolegend), BV605 anti Sca-1 (D7, 108134, Biolegend), BV785 anti c-Kit (2B8, 105841, Biolegend), AF700 anti CD34 (RAM34, 560518, BD), PE anti FLK2 (A2F10, 135306, Biolegend), APC-Cy7 anti CD48 (HM48-1, 103432, Biolegend), PE-dazzle 594 anti CD150 (TC15-12F12.2, 115936, Biolegend), FITC anti CD16/32 (93, 101306, Biolegend), BV650 anti CD115 (T38-320, 743641, BD), APC-R700 anti CD45 (30-F11, 565478, BD), APC-Cy7 anti F4/80 (BM8, 123118, Biolegend), PE-dazzle 594 anti PD-L2 (TY25, 107216, Biolegend), BV650 anti CD206 (C068C2, 141723, Biolegend), FITC anti IL-10 (JES5-16E3, 505006, Biolegend), PE-Cy7 anti CD11b (M1/70, 25-0112-82, eBioscience), APC anti Ly-6G

(1A8, 561236, BD Biosciences), BV421 anti Ly-6C (AL-21, 562727, BD Biosciences). Antibodies were purchased from BD biosciences, Biolegend, and Abcam. Flow cytometric data were acquired by a LSRFortessa™ cytometer (BD Biosciences, San Jose, CA) and were analyzed using FlowJo 10 (TreeStar).

Drug treatment

PLX3397

In vivo depletion of microglia was achieved by daily administration of a colony stimulating factor 1 receptor inhibitor PLX3397 as previously published[95, 102-104]. PLX3397 (Selleckchem, Houston, TX) was dissolved in DMSO administered daily through oral gavage at a dose of 40 mg/kg for 21 days. ICH was induced following 21 days, and daily administration regime continued until experimental endpoints.

Tamoxifen

Tamoxifen (Sigma-Aldrich) was dissolved in ethanol/corn oil (1:9) at a concentration of 30 mg/mL, mice were injected intraperitoneally with 100 µL (3 mg/mouse) daily for 5 consecutive days prior to induction of models.

β3-adrenergic receptor agonist and antagonist

SR59230A, a selective antagonist for β3-adrenergic receptor was purchased from Sigma-Aldrich, and dissolved in PBS. Mice were injected with the SR59230A intraperitoneally twice daily at a dose of 5 mg/kg body weight. SR59230A was administered immediately after model induction till sacrifice. Mirabegron, a selective agonist for β3-adrenergic receptor was purchased from Medchem, was dissolved in DMSO/PBS (1:9). Mirabegron was given to mice via daily oral gavage at a dose of 2 mg/kg. Mirabegron treatment was initiated immediately after model induction till the end of experiment.

Recombinant IL-3

Recombinant IL-3 was obtained from STEMCELL Technologies. IL-3 was injected intraperitoneally to mice at a dose of 600ng/mouse daily immediately after ICH induction till the end of experiment.

Transcriptome sequencing of Mouse HSCs

$Lin^-Sca\text{-}1^+c\text{-}kit^+CD34^-FLK2^-CD48^-CD150^+$ HSCs were sorted from bone marrow of ICH and sham mice at day 3 after surgery. Cell sorting was completed on a FACS ARIA™ II cytometer (BD Biosciences, San Jose, CA) after labeling with antibodies. Cells were directly sorted into Trizol LS, and RNA was then extracted. Transcriptome sequencing was conducted by Nanostring with a mouse immunology panel, data were analyzed by nSolver4.0 (Nanostring).

Immunostaining

Immunohistochemistry staining of mice and ICH patient post-mortem brain tissue were conducted as we described previously[5, 105].The following primary antibodies were used: rabbit anti mouse/human GFAP (1:1000, Abcam), goat anti human IL-15 (1:50; Santa Cruz Biotechnology), goat anti mouse Iba1 (1:500, Abcam). Primary antibody was incubated at 4°C overnight followed by incubation with Alexa Fluor 594 or 488 conjugated donkey anti-rabbit or goat secondary antibody (1:1000, Thermo Fisher Scientific) for 1 hour at room temperature. Images were captured by a confocal microscope and analyzed by ImageJ.

Statistical Methods

Standard power calculations to determine sample size that results in statistically significant differences were calculated at $\alpha = 0.05$ and a power of 0.8. Power analysis and sample size calculations were performed using SAS 9.1 software (SAS Institute Inc. Cary, NC, USA), based on our experience with the respective tests, variability of the assays and inter-individual differences among experimental groups. Animals were randomly assigned to experimental groups. Randomization was based on the random number generator function in Microsoft Excel. Investigators who evaluated the outcome and processed data were masked to the experimental

groups. For gene profiling of HSCs, cells were sorted from 5 mice and pooled as a single biological sample. All experiments presented in this study were repeated at least three times. A two-tailed unpaired Student's *t* test was used to compare between two independent groups. One-way Analysis of variance (ANOVA) followed by Tukey post hoc test was used to compared three or more groups with one variable. For comparison of two or more variables among multiple groups, two-way ANOVA followed by Bonferroni post hoc test were used. Data are expressed as mean ± SEM. $P < 0.05$ was considered significant. Statistical analyses were performed using Prism 7.0 software (GraphPad, San Diego, CA, USA).

INTERLEUKIN-15 BRIDGES ASTROCYTE-MICROGLIA CROSSTALK AND EXACERBATES BRAIN INJURY FOLLOWING INTRACEREBRAL HEMORRHAGE

Robust upregulation of IL-15 in astrocytes following ICH in humans and mice

Astrocytes are identified as a major contributor to neuroinflammation and source of IL-15 in the CNS[66, 93]. To determine whether human astrocytes are a relevant source of IL-15 in the setting of ICH, we assessed the expression of IL-15 in human astrocytes of postmortem brain tissues from patients with ICH[106]. The number of IL-15$^+$ astrocytes was dramatically increased by approximately six folds in the perihematomal area of ICH patients as compared to non-neurological controls (**Figure 4A-B**). Notably, astrocytes in the ICH brain display enlarged somas and increased processes (**Figure 4A**). Similar findings were seen in a murine ICH model induced by collagenase injection. Flow cytometry analysis revealed that astrocytes are the major cellular source of IL-15 in the hemorrhagic brain of wild type (WT) mice at day 1 after ICH onset (**Figure 4C-D**). These results indicate that ICH induces rapid upregulation of IL-15 in astrocytes.

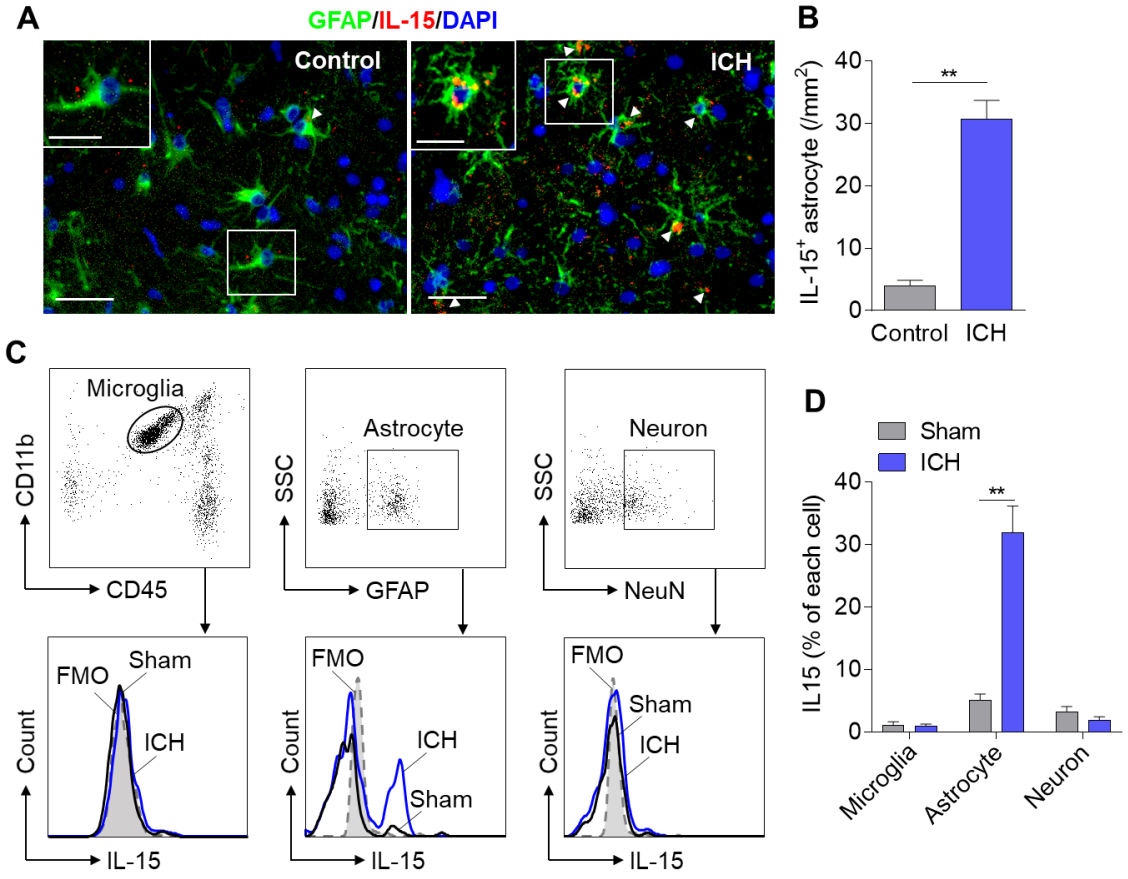

Figure 4. Upregulation of astrocytic IL-15 after ICH in humans and mice.

(**A**) Images show the expression of IL-15 in astrocytes in the perihematomal region of brain sections from an ICH patient and a control subject without neurological disease. Arrow heads: IL-15^{+} astrocytes. Scale bar = 100 μm, and 50 μm in insets. (**B**) Quantification of IL-15^{+} astrocytes in brain sections. n = 18 per group from 6 ICH patients or 6 controls. (**C-D**) ICH was induced in wild type C57BL/6 mice via collagenase injection. Flow cytometry analysis of brain cells expressing IL-15 was conducted at day 1 after ICH. (**C**) Flow cytometry gating strategy of microglia (CD45^{low}CD11b^{+}), astrocytes (GFAP^{+}), and neurons (NeuN^{+}), and histograms showing their expression of IL-15. (**D**) Quantification of IL-15 expression by indicated groups of brain cell types after ICH. n = 12 per group. Data are shown as mean ± SEM, ** $P < 0.01$.

Astrocyte-targeted expression of IL-15 exacerbates hemorrhagic brain injury in mice.

To investigate the potential involvement of astrocyte-derived IL-15 in ICH injury, a transgenic mouse line where over-expression of IL-15 is targeted to astrocytes by a glial fibrillary acidic protein (GFAP) promoter (GFAP-IL-15^{tg}) was generated in our lab (**Figure 5**). As we previously reported[69, 93], GFAP-IL-15^{tg} mice develop normally without clinical sign of neurological disease or behavioral abnormalities. Moreover, astrocyte-targeted expression of IL-15 did not affect neurovascular function nor prompt systemic immune responses, suggesting that the overproduction of IL-15 is restricted to the CNS without notable effects on brain inflammation under physiological conditions[93]. ICH was induced by collagenase injection. At days 1 and 3 following ICH, GFAP-IL15^{tg} mice exhibited worsened neurologic deficits reflected by higher mNSS scores relative to their WT littermates (**Figure 6A**). GFAP-IL15^{tg} mice had similar hematoma volume compared to their WT littermates (**Figure 6B-C**). However, perihematomal edema (PHE) volume was dramatically increased in GFAP-IL15^{tg} mice at days 1 and 3 after ICH (**Figure 6B-C**). Notably, GFAP-IL15^{tg} mice also showed increased brain water content relative to their WT littermates at day 3 after ICH (**Figure 6D**). Similarly, in an autologous blood injection ICH model, exacerbated neurodeficits as well as augmented brain edema in GFAP-IL-15^{tg} mice was also recorded (**Figure 7**). Of interest, I found insignificant alterations of hyperintense areas in diffusion-weighted images (DWI) images of GFAP-IL-15^{tg} mice versus WT mice after ICH (**Figure 8**). In contrast, a significant increase in T2 values was noted in GFAP-IL-15^{tg} mice versus WT mice after ICH (**Figure 8**). These results suggest that vasogenic edema contributes to the augmented brain edema in GFAP-IL-15^{tg} mice following ICH.

To ascertain the direct effects of IL-15, I next examined the impact of antibody neutralization of IL-15, as well as knockdown of astrocytic IL-15, on ICH injury in wild type mice. In these experiments, reduction in neurodeficits and brain edema in wild type ICH mice subjected to antibody neutralization of IL-15, or knockdown of astrocytic IL-15, was found (**Figure 9**).

Together, these experimental results demonstrate that astrocytic IL-15 exacerbates brain injury following ICH in mice.

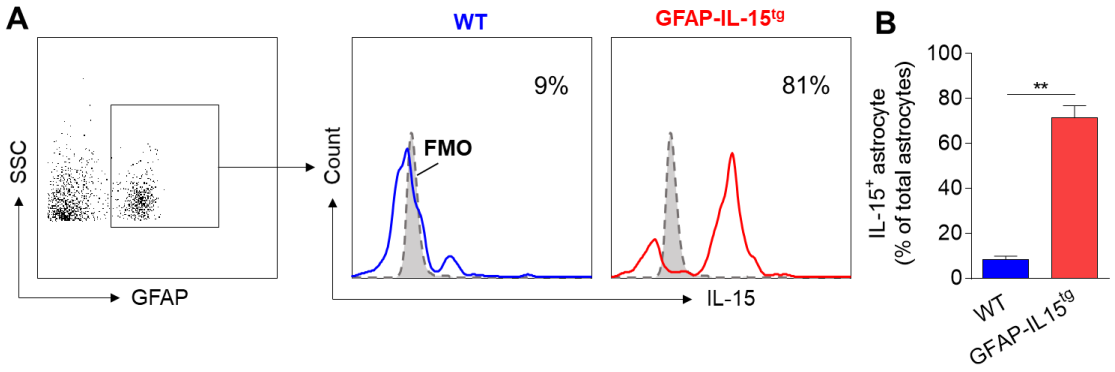

Figure 5. Astrocyte-targeted expression of IL-15 in GFAP-IL-15^{tg} mice. (**A**) Flow cytometry dot plots show the gating of GFAP^{+} astrocytes and histograms show the expression of IL-15 by WT and GFAP-IL-15^{tg} mice astrocytes. (**B**) Quantification of IL-15^{+} astrocytes. Data are presented as mean ± SEM. n = 6 ** P < 0.01.

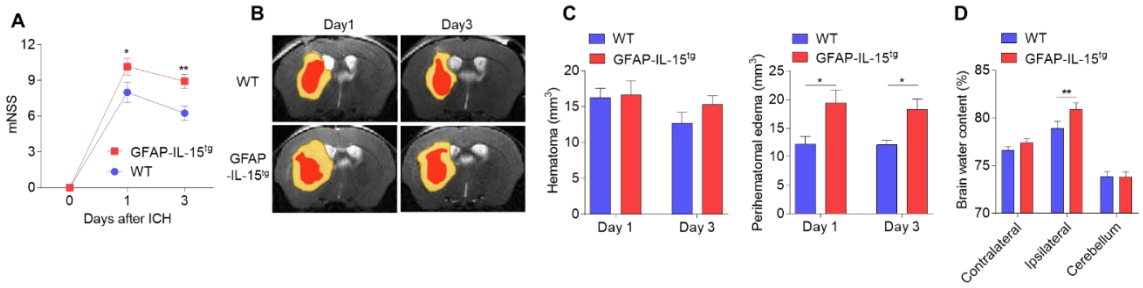

Figure 6. Astrocyte-targeted expression of IL-15 exacerbates hemorrhagic brain injury.
ICH was induced by collagenase injection in groups of GFAP-IL-15^{tg} and wild type (WT) mice. (**A**) Neurodeficits were evaluated at baseline, day 1 and day 3 after ICH. n = 12 in WT group; n = 14 in GFAP-IL-15^{tg} group. (**B**) MRI images show hematoma (red) and perihematomal edema (yellow) in groups of WT and GFAP-IL-15^{tg} mice at days 1 and 3 after ICH. (**C**) Quantification of hematoma volume and perihematomal edema of 7T MRI. n = 8 per group. (**D**) Quantification of

brain water content in groups of WT and GFAP-IL-15^{tg} mice at day 3 after ICH. n = 8 per group. Data are presented as mean ± SEM. * $P < 0.05$, ** $P < 0.01$.

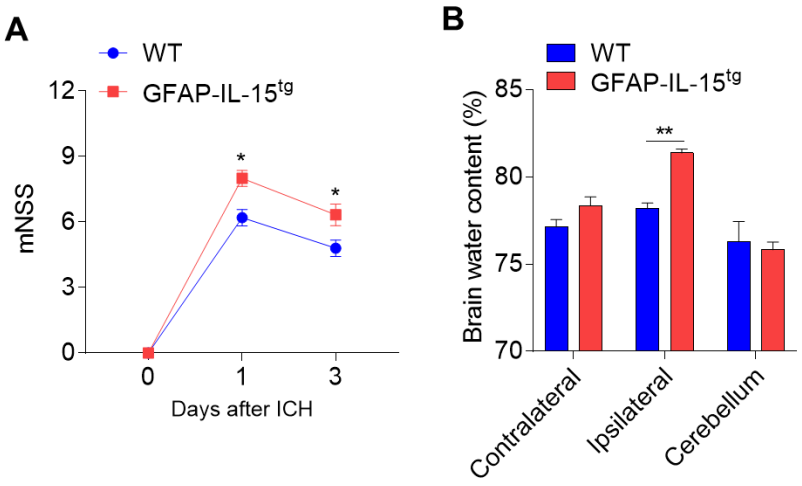

Figure 7. Effects of astrocyte-targeted expression of IL-15 on hemorrhagic brain injury in autologous blood injection model.

ICH was induced by intracerebral injection of autologous blood in wild type and GFAP-IL-15^{tg} mice. (**A**) Neurodeficits were assessed at days 1 and 3 after ICH induction using mNSS score. (**B**) Brain water content was measured at day 3 after model induction in WT and GFAP-IL-15^{tg} mice. n = 7 in WT group and n = 6 in GFAP-IL-15^{tg} group. Data are presented as mean ± SEM. * $P < 0.05$, ** $P < 0.01$.

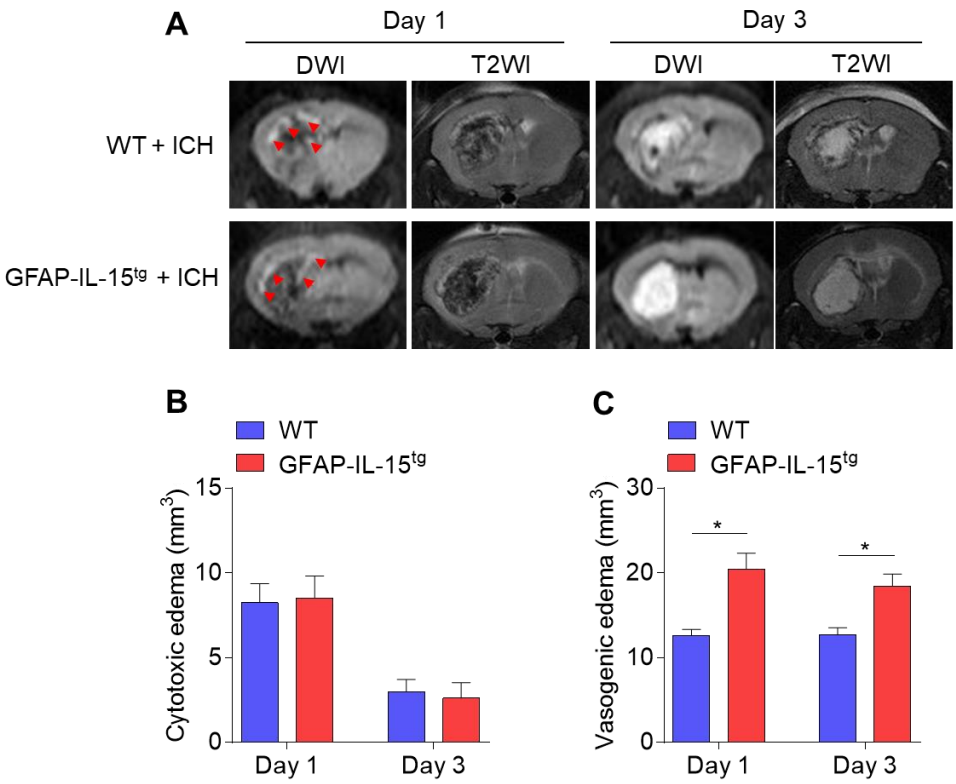

Figure 8. Effects of astrocyte-targeted expression of IL-15 on brain edema after ICH.

ICH was induced by collagenase injection in wild type and GFAP-IL-15^{tg} mice. Cytotoxic and vasogenic brain edema was evaluated by MRI DWI and T2WI scans, respectively. (**A**)**.** Brain DWI and T2WI images of wild type and GFAP-IL-15^{tg} mice at days 1 and 3 after ICH. Red arrows: hyperintensity signals in DWI images indicating cytotoxic edema. (**B-C**)**.** Quantification of cytotoxic edema area and vasogenic edema area. Data are presented as mean ± SEM. * $P <$ 0.05.

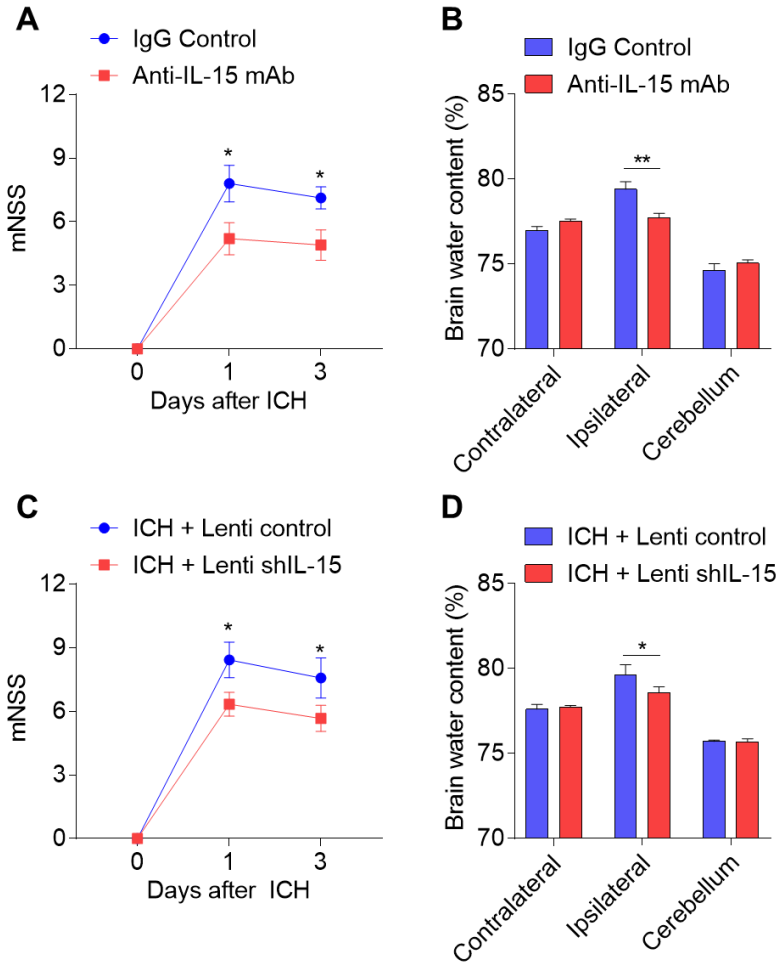

Figure 9. Effects of IL-15 neutralization or knockdown of astrocytic IL-15 on ICH injury in WT mice.

ICH was induced by collagenase injection in WT mice. (**A-B**) Anti-IL-15 mAb or IgG control was given immediately after ICH induction via intraventricular injection. Neurodeficits were evaluated at day 1 and day 3 after ICH (**A**). Brain water content was quantified at day 3 after ICH (**B**). n = 8 per group. (**C-D**) To knockdown astrocytic IL-15 *in vivo*, we used a lentivirus vector containing GFAP-shIL-15, in which GFAP promotor controls the transcript of a small hairpin RNA that silences IL-15 expression. ShIL-15 or control lentivirus was injected into the right hemisphere of WT mice. ICH was induced by collagenase injection at day 5 after lentivirus injection. (**C**) Neurodeficits were evaluated at days 1 and 3 after ICH. (**D**) Brain water content was measured at

day 3 after ICH induction. n = 8 per group. Data are presented as mean ± SEM. * $P < 0.05$, ** $P < 0.01$.

Astrocyte-targeted expression of IL-15 skews microglia towards a proinflammatory phenotype after ICH

Considering the key role of IL-15 in the regulation of inflammatory responses, which extensively contribute to blood-brain barrier disruption and PHE expansion in ICH[4, 60, 95], I subsequently investigated the impact of astrocytic IL-15 on the profile of immune cells within the ICH brain. At day 3 after ICH, the numbers of microglia and brain-infiltrating immune cell subsets were evaluated by flow cytometry. A similar number of brain-infiltrating neutrophils, macrophages, T- and B cells, were counted in the ICH brain tissues obtained from groups of WT and GFAP-IL-15^{tg} mice (**Figure 10A-B**). In contrast, the count of microglia was dramatically increased in GFAP-IL-15^{tg} mice (**Figure 10A-B**). Immunostaining results revealed an abundant accumulation of microglia in the perihematomal area within the proximity to astrocytes in brain sections of GFAP-IL-15^{tg} mice obtained at day 3 after ICH (**Figure 11A-B**). These microglia possessed enlarged cell soma and retracted processes (**Figure 11A**). Flow cytometry analysis of microglia revealed a robust upregulation of activation marker CD86, IL-1β, and TNF-α in GFAP-IL-15^{tg} mice after ICH (**Figure 11C-D**). These results indicate that astrocytic IL-15 predominantly impacts microglial response rather than other immune cell subsets, and skews microglia response towards a pro-inflammatory phenotype following ICH.

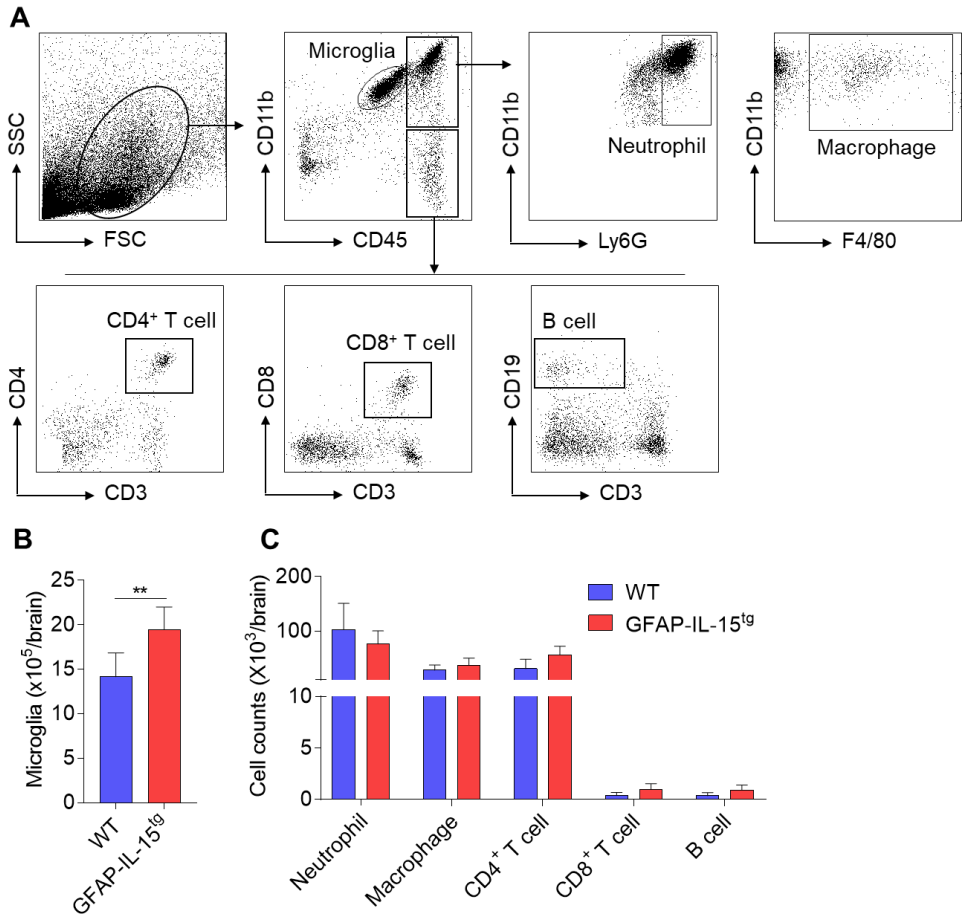

Figure 10. Augmented microglia response in GFAP-IL-15^{tg} mice after ICH.

ICH was induced by collagenase injection in groups of GFAP-IL-15^{tg} and WT mice. Flow cytometry analysis of brain tissues were conducted at day 3 after ICH. (**A**) Flow cytometry gating strategies of microglia (CD45^{low}CD11b^{+}), neutrophils (CD45^{hi}CD11b^{+}Ly6G^{+}), macrophages (CD45^{hi}CD11b^{+}F4/80^{+}), CD4^{+} T cells (CD45^{hi}CD3^{+}CD4^{+}), CD8^{+} T cells (CD45^{hi}CD3^{+}CD8^{+}), and B cells (CD45^{hi}CD3^{-}CD19^{+}). (**B**) Quantification of microglia number in brain tissues obtained from groups of WT and GFAP-IL-15^{tg} mice at day 3 after ICH. (**C**) Quantification of infiltrating immune cells in brain tissues obtained from groups of WT and GFAP-IL-15^{tg} mice at day 3 after ICH. Data are presented as mean ± SEM. n = 8 per group. ** $P < 0.01$.

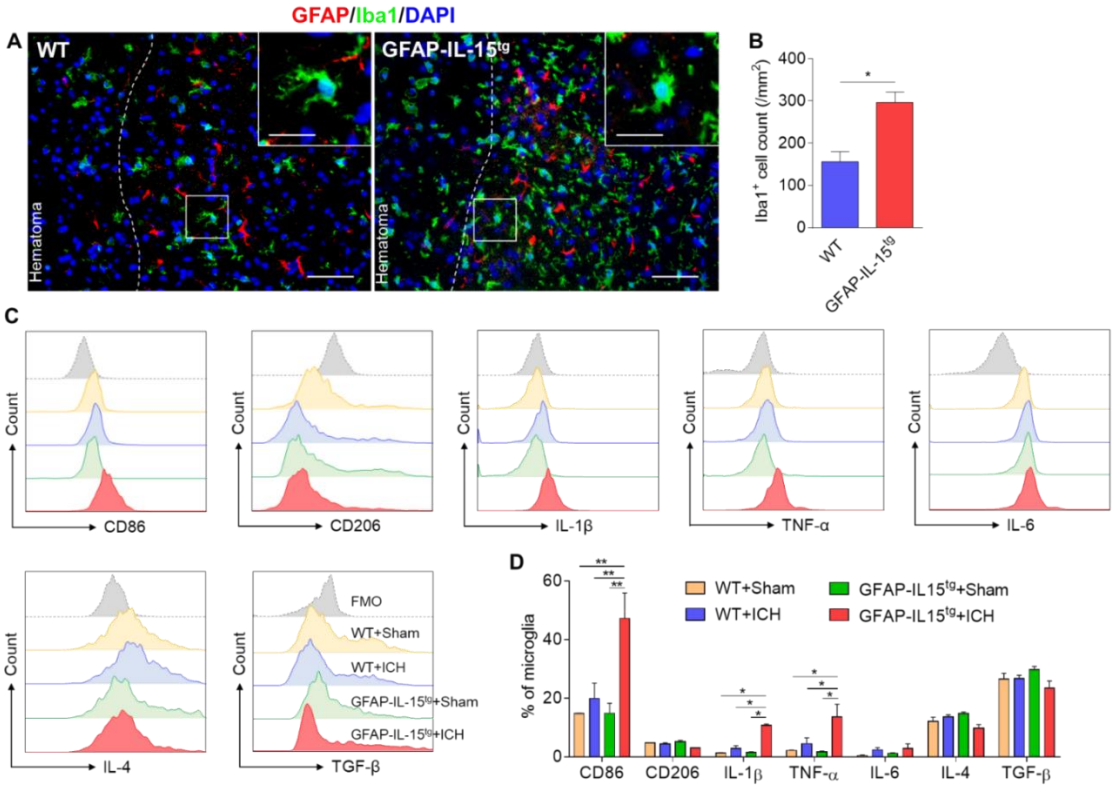

Figure 11. Skewed microglia response toward a proinflammatory phenotype in GFAP-IL-15^{tg} mice after ICH.

ICH was induced by collagenase injection in GFAP-IL-15^{tg} and WT mice. (**A**) Immunofluorescent images showing astrocytes and microglia in the perihematomal region of brain sections obtained from WT and GFAP-IL-15^{tg} mice at day 3 after ICH. Dashed lines indicate the borders of hematoma. Insets showing single microglia. Scale bar = 100 μm, and 20 μm in insets. (**B**) Quantification of microglia in the perihematomal area. n = 16 from 4 mice per group. (**C**) Histograms showing the expression of indicated markers by microglia in indicated groups of mice at day 3 after ICH. (**D**) Quantification of expression of indicated markers in **C**. n = 8 per group. Data are presented as mean ± SEM. * $P < 0.05$, ** $P < 0.01$.

Microglial depletion ablates the augmentation of hemorrhagic injury in GFAP-IL-15^{tg} mice

To determine the involvement of microglia in the augmentation of ICH injury by astrocyte-derived IL-15, I compared the effects of microglia depletion on neurological deficits and brain edema in

groups of WT and GFAP-IL-15^{tg} mice. A colony stimulating factor 1 receptor (CSF1R) inhibitor PLX3397 was administered to deplete microglia in mice, as previously described[95, 103, 104]. Daily administration of PLX3397 for 3 consecutive weeks led to an approximate 80% reduction of microglia in the brain (**Figure 12A**). At day 21 of PLX3397 administration, ICH was induced by collagenase injection; PLX3397 treatment continued until the end of experiments. Similar levels of neurodeficits and brain edema were observed in groups of WT and GFAP-IL-15^{tg} mice receiving PLX3397 (**Figure 12B-C**), suggesting that ablation of microglia diminishes the augmentation of ICH injury by astrocytic IL-15.

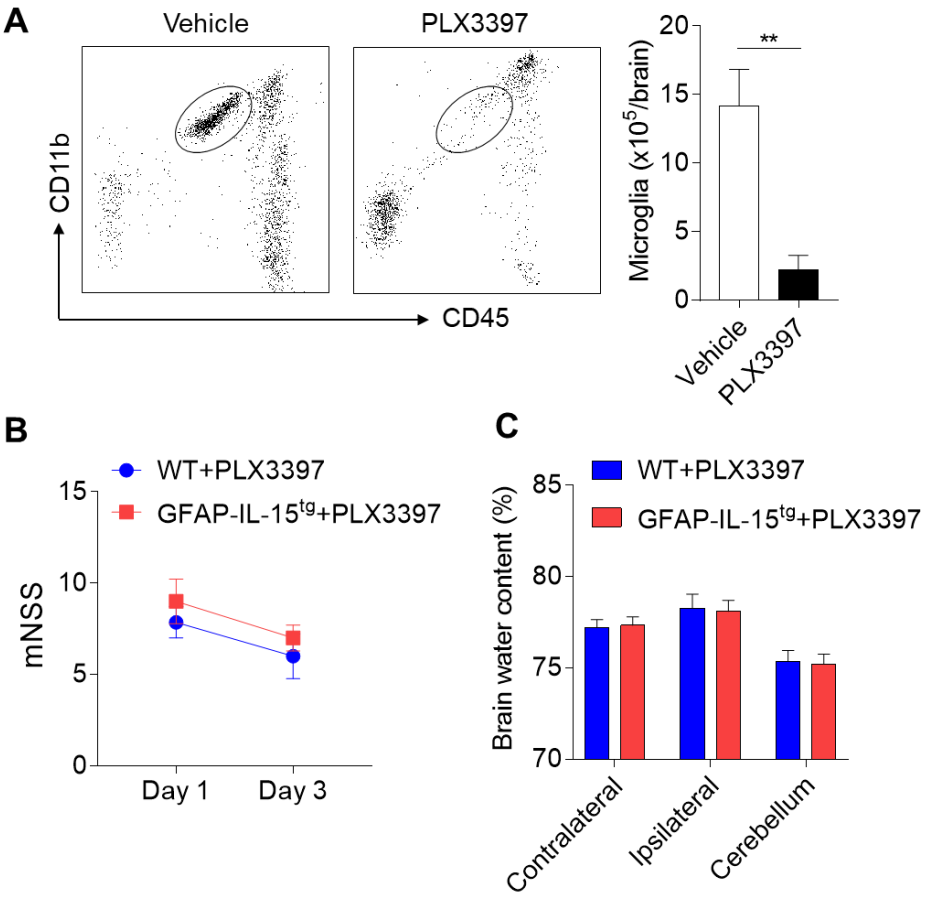

Figure 12. Depletion of microglia diminishes the exacerbation of ICH injury in GFAP-IL-15^{tg} mice. GFAP-IL-15^{tg} and wild type (WT) mice received oral gavage of PLX3397 or vehicle daily at a dose of 40 mg/kg for 21 days and followed by collagenase injection. PLX3397 treatment

continued until the end of experiments. (**A**) Flow cytometry gating strategy and quantification showing microglia numbers in the brain tissues obtained from indicated groups of mice receiving vehicle or PLX3397 for 21 days. n = 6 per group. (**B**) Neurological deficits were evaluated by mNSS at days 1 and 3 after ICH. n = 12 per group. (**C**) Quantification of brain water content at day 3 after ICH. n = 12 per group. Data are shown as mean ± SEM. ** $P < 0.01$.

Summary

- ICH induces upregulation of IL-15 in astrocytes.
- Astrocyte-targeted expression of IL-15 exacerbates ICH injury.
- Astrocyte-derived IL-15 skews microglia toward a proinflammatory phenotype following ICH.
- Astrocytic IL-15-induced augmentation of microglial response contributes to ICH injury.

CHAPTER 5

BRAIN INJURY INSTRUCTS BONE MARROW CELLULAR LINEAGE DESTINATION THAT SUPPRESSES NEUROINFLAMMATION

ICH swiftly activates bone marrow hematopoietic response in humans

After ICH Leukocytes in the circulation and immune organs are mobilized, leading to pronounced infiltration of myeloid cells into the hemorrhagic brain after ICH[78, 107-109]. Due to the rapid turn-over rate of myeloid cells, the limited leukocyte supply from cell reservoirs are rapidly depleted, stimulating the replenishment of new cells from HSCs and progenitor cells in hematopoietic organs. Therefore, we obtained bone marrow cells by flushing out cranial bone flaps removed during decompressive surgery in ICH patients during the acute stage to investigate their response. This novel approach in accessing bone marrow cells allows us to directly assess the response of HSCs to ICH in human patients. Notably, an apparent increase in HSC count was observed (**Figure 13A-B**), in conjunction with a sharp increase of downstream myeloid cell progenitors (**Figure 13C-D**) in patient derived bone marrows as compared to controls. In contrast, the numbers of downstream lymphoid cell progenitors were not impacted in patient derived samples. These results suggest that ICH increases HSC activity and shifts hematopoiesis towards the myeloid cell lineages in ICH patients.

Given this striking observation in patient samples, I then investigated the bone marrow cell response in a collagenase mouse model of ICH. Activity of bone marrow resident cells in mice spine vertebrae was evaluated by micro-PET scanning at 1 hour after ^{18}F-FDG injection 3 days post-ICH. Uptake of ^{18}F-FDG in bone marrow was significantly increased in ICH mice as compared to sham controls (**Figure 14**). Moreover, bone marrow collected from femur bones were evaluated for the counts of $Lin^{-}Sca\text{-}1^{+}cKit^{+}$ (“LSK”) cells (a classic signature of HSCs) and of long-term self-renewing HSCs ($Lin^{-}Sca\text{-}1^{+}cKit^{+}CD34^{-}FLK2^{-}CD48^{-}CD150^{+}$). A dramatic increase of LSK cells and long-term self-renewing HSCs at day 3 after ICH and corresponding increase in

proliferation is recorded (**Figure 15**). These data indicate that ICH increases bone marrow hematopoietic activity.

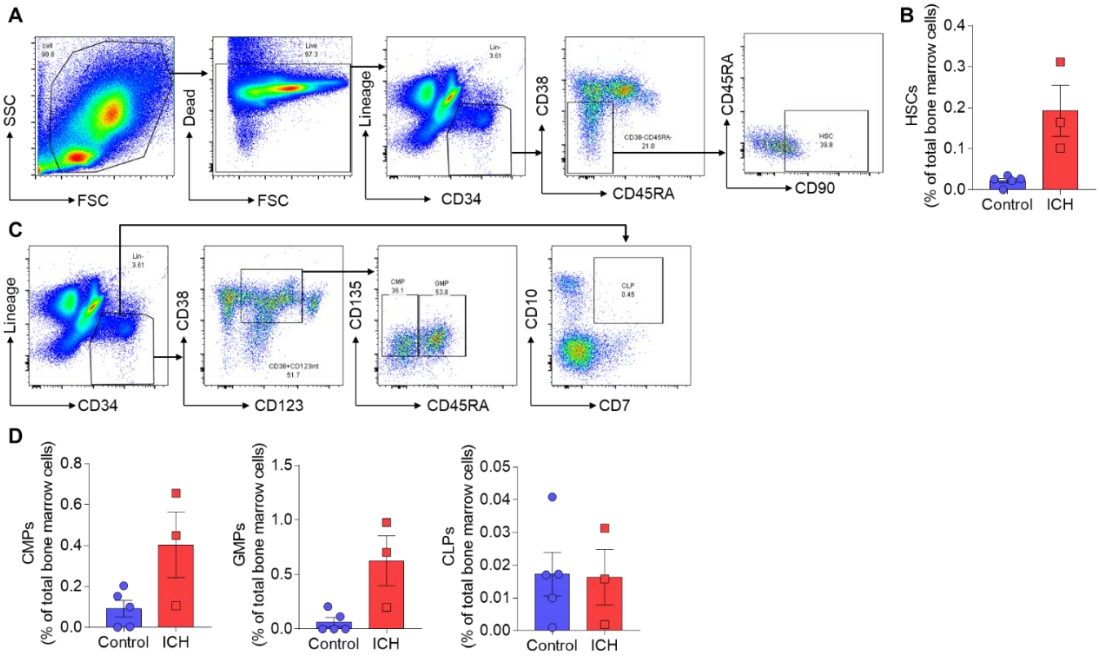

Figure 13. ICH induces a swift response in bone marrow of ICH patients.

Bone marrow cells were flushed out from cranial bone flaps obtained from ICH patients at an average time of 22 ± 11 hours post-ictus. Bone marrow cells obtained from cranial bone flaps of patients undergoing microsurgical clipping of unruptured brain aneurysm were used as controls. **A.** Gating strategy for human bone marrow HSCs ($Lin^-CD34^+ CD90^+ CD38^- CD45RA^-$). **B.** Bar graph shows the increase of HSCs (% of total bone marrow cells) following ICH. **C.** Gating strategy for myeloid progenitors ($CD34^+ CD123^{low} CD38^+ CD135^+ CD45RA^-$), granulocyte monocyte progenitors ($CD34^+ CD123^{low} CD38^+ CD135^+ CD45RA^+$) and common lymphoid progenitors ($CD34^+ CD7^+ CD10^+$). **D.** ICH-induced increase of myeloid progenitors but not lymphoid progenitors (% of total bone marrow cells) in the bone marrow of ICH patients. n = 3 in ICH, n = 5 in control. Mean ± SEM.

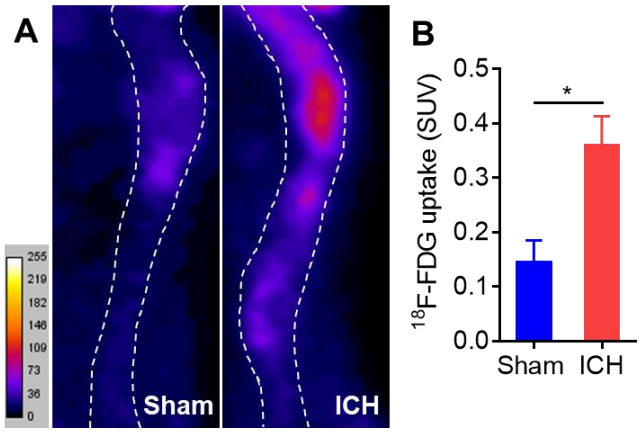

Figure 14. ICH increases bone marrow uptake of ^{18}F-FDG.

ICH was induced in 3-month old male mice by collagenase injection, **^{18}**F-FDG PET scan was performed at day 3 after ICH. (**A**) PET images show **^{18}**F-FDG uptake in the spinal column of sham and ICH mice, dashed lines show the position of spinal column. (**B**) Quantification of standard uptake volume (SUV). Mean ± SEM, n = 8 per group, **P* < 0.05.

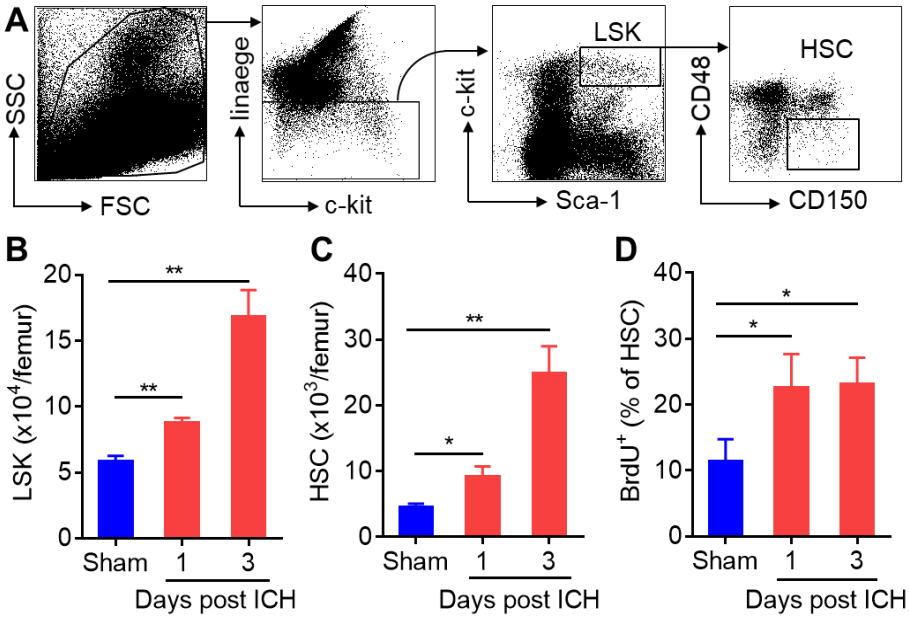

Figure 15. ICH increases bone marrow HSC activity.

ICH was induced in 3-month old male mice by collagenase injection, saline injected mice were used as control. BrdU was injected i.p. 1 day before sacrifice at the dosage of 150 mg/kg. At days 1 and 3 after ICH, bone marrow cells were collected from femur and assessed by flow cytometry. (**A**) Gating strategies show the gating of LSK cells ($Lin^-c\text{-}Kit^+Sca\text{-}1^+$) and HSCs ($Lin^-c\text{-}Kit^+Sca\text{-}1^+CD34^-FLK2^-CD48^-CD150^+$). (**B-C**) Quantification of cell number of LSKs (**B**), HSCs (**C**) and BrdU incorporation by HSCs (**D**). mean ± SEM. n = 12 per group. **P* < 0.05, ***P* < 0.01.

ICH induces myeloid bias of bone marrow HSCs with increased production of Ly6C^{low} monocytes

To fate-map the hematopoiesis of mice after ICH a Fgd5-CreER-tdTomato mouse line was adopted, where HSCs and their downstream cell lineages express tdTomato upon activation of Cre via tamoxifen treatment in $Fgd5^+$ HSCs (**Figure 16A**). The use of this mouse line allows for the tracking of HSCs activity along with their downstream cell lineages. In Fgd5-CreER-tdTomato mice, tamoxifen regimen was administered for 5 days to evoke tdTomato expression in HSCs, mice were then subjected to ICH induction. Cell counts of $tdTomato^+$ cells in HSCs, progenitors, and mature leukocyte subsets were measured by flow cytometry at day 3 after ICH. Following ICH, a two-fold increase of $tdTomato^+$ HSCs was quantified in the bone marrow, accompanied by a shift of bone marrow hematopoiesis towards myeloid cells (**Figure 16B-C**). Myeloid cell proliferation was also characterized by a sharp increase of myeloid progenitors [granulocyte-monocyte progenitors (GMPs) and monocyte-dendritic cell progenitors (MDPs)] (**Figure 16C**). As a result, the population of $Ly6C^{low}$ monocytes were predominantly increased, rather than those of neutrophils and lymphocytes (**Figure 16C**).

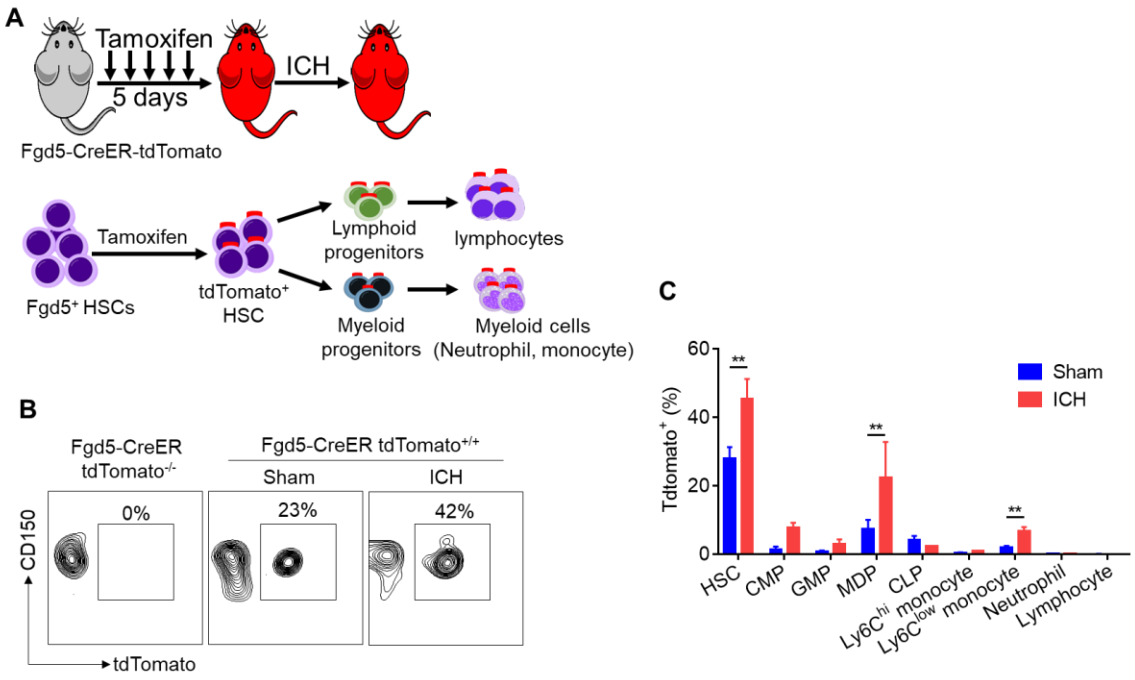

Figure 16. Lineage tracing of genetically labeled HSCs and their fate in ICH mice.

(**A**) Schematic shows tamoxifen injection and ICH induction in Fgd5-creER-tdTomato mice. Fgd5 is shown to be specifically expressed in HSCs, Fgd5-CreER allele exhibits inducible CreER activity exclusively in self-renewing HSCs. These HSCs and their downstream lymphoid/myeloid cell types are all tdTomato+ after tamoxifen induction. New HSCs, progenitors and mature cells were evaluated in bone marrow at day 3 after ICH. (**B**) Flow cytometry gating strategy of newly generated tdTomato⁺ HSCs in bone marrow. (**C**) Quantification of tdTomato⁺ cell percentage in subpopulations of HSCs, myeloid and lymphoid progenitors, differentiated myeloid cells and lymphocytes. Mean ± SEM. n = 6 per group. $^{**}P < 0.01$.

Newly emergent Ly6C^{low} monocytes accumulate in the ICH brain and highly express anti-inflammatory factor IL-10.

To understand whether increased bone marrow production of Ly6C^{low} monocytes leads to the outflow of these cells from bone marrow and subsequent migration into the injured brain, the count of tdTomato^{+} cells in the brain of Fgd5-CreER-tdTomato mice at day 3 after ICH were quantified using flow cytometry. A robust increase in newly emerged tdTomato^{+}Ly6C^{low} monocytes and their tdTomato^{+} macrophage descendants were discovered in the brain of ICH mice (**Figure 17A**). In the ICH mouse brain, both tdTomato^{+}ly6C^{low} monocytes and tdTomato^{+} macrophage derivatives highly expressed IL-10 relative to their tdTomato^{-} cell subsets (**Figure 17B**). Notably, tdTomato^{+} macrophages highly expressed "alternative activation" markers CD206 and PD-L2 (**Figure 17C**). These data suggest that the newly generated anti-inflammatory Ly6C^{low} monocytes can home to the brain of ICH mice and thereafter differentiate into "alternatively activated" macrophages, and potentially may promote hematoma clearance and ICH recovery.

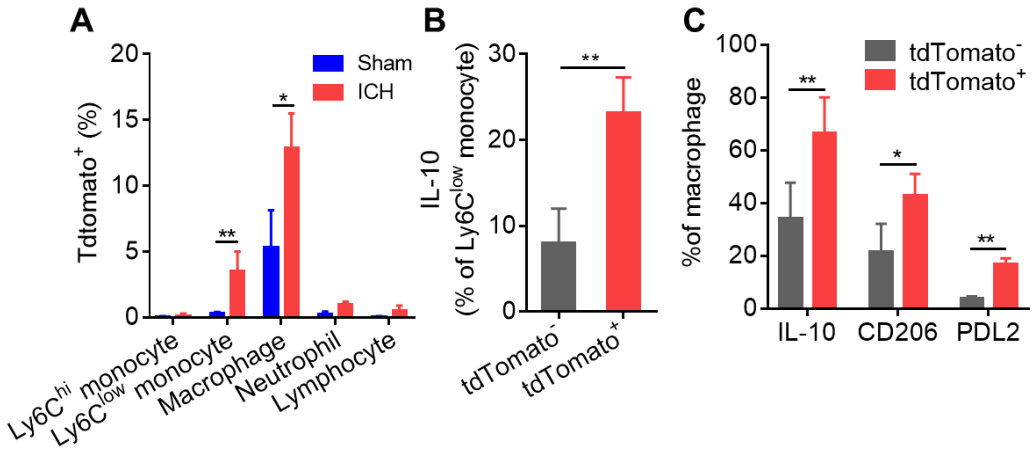

Figure 17. Newly emerged Ly6C^{low} monocytes transmigrate to the brain of ICH mice.

(**A**) Quantification of tdTomato^{+} immune cell subsets in the brain of Fgd5-creER-tdTomato mice at day 3 post ICH. (**B**) Newly generated (tdTomato^{+}) Ly6C^{low} monocytes in the ICH brain highly express IL-10. (**C**) Newly generated tdTomato^{+} macrophages in the ICH brain highly express IL-

10 and alternative activation markers (CD206 and PDL2). Mean ± SEM, n = 6 per group. *P < 0.05, **P < 0.01.

Increased sympathetic tone induces bone marrow hematopoiesis response after ICH

Hematopoiesis activity is delicately regulated by neurogenic signals[110]. Activity of the sympathetic nervous system (SNS) is hypothesized to activate bone marrow HSCs in through β3-adrenergic receptors innervation of the bone marrow niche[111]. Norepinephrine, a systemic SNS neurotransmitter, is upregulated in both ICH patients and corresponding animal models[4]. Therefore, here I tested whether increased adrenergic input mediated the hematopoietic response following ICH by administering an adrenergic antagonist. Bone marrow HSC counts were reduced by approximately two-fold at day 3 after ICH in mice treated with a selective β3-adrenergic receptor antagonist, SR59230A (**Figure 18A**). Moreover, in treated mice the proliferation ability measured by HSC BrdU incorporation was also significantly inhibited by blockade of the β3-adrenergic receptor (**Figure 18A**). Myeloid progenitors in the bone marrow similarly decreased in count upon treatment (**Figure 18B**). These data indicate that increased sympathetic tone after ICH activates bone marrow hematopoiesis.

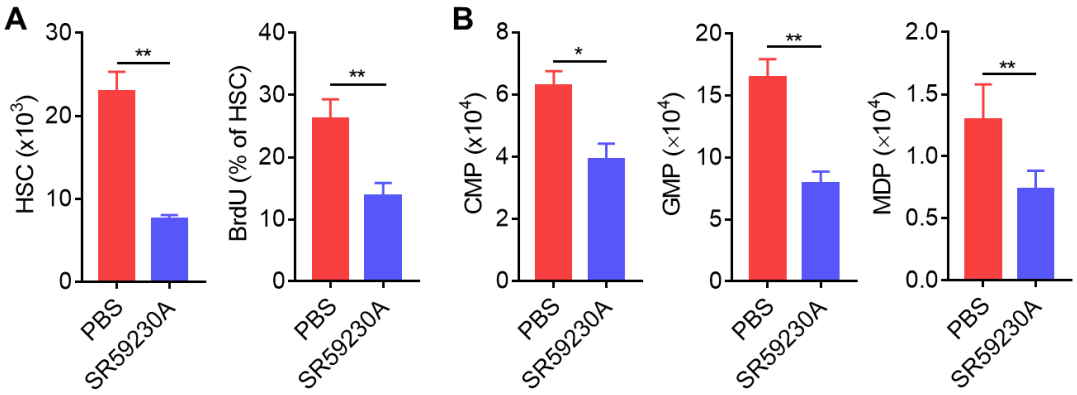

Figure 18. Blockade of adrenergic β3 receptor diminishes ICH-induced increase of HSC activity in bone marrow.

ICH was induced by collagenase injection in 3 month old male C57BL/6J mice. Adrenergic β3 receptor antagonist SR59230 (5 mg/kg) was given intraperitoneally immediately after ICH induction, twice daily. Bone marrow was obtained from femoral bones of ICH or sham mice 3 days after surgery. Flow cytometry was conducted to evaluate the bone marrow response. (A) HSC number and incorporation of BrdU. (B) Cell counts of myeloid progenitors at day 3 after ICH. N = 8 per group. Mean ± SEM. *P < 0.05, **P < 0.01.

Upregulation of small RhoGTPase Cdc42 in bone marrow HSCs after ICH.

The hematopoietic activity of HSCs is tightly controlled by their intracellular machinery[112, 113]. High-throughput Nanostring screening of the HSC transcriptome was used to identify the molecular characteristics of bone marrow-derived HSCs in response to ICH. Unbiased analysis of HSCs sorted from mouse femurs 3 days post-ICH identified a drastic upregulation of the small Rho-GTPase Cdc42 in the HSC transcriptome, specifically, the Cdc42 gene was altered in HSCs of ICH mice relative to control (**Figure 19A**). To evaluate the activity of Cdc42 of HSCs after ICH, consistent to the transcriptomic sequencing data, flow cytometry reveals that active Cdc42 was increased in HSCs of ICH mice at day 3 after model induction (**Figure 19B, C**). Cdc42 has been causally linked to myeloid bias of HSCs[114, 115].

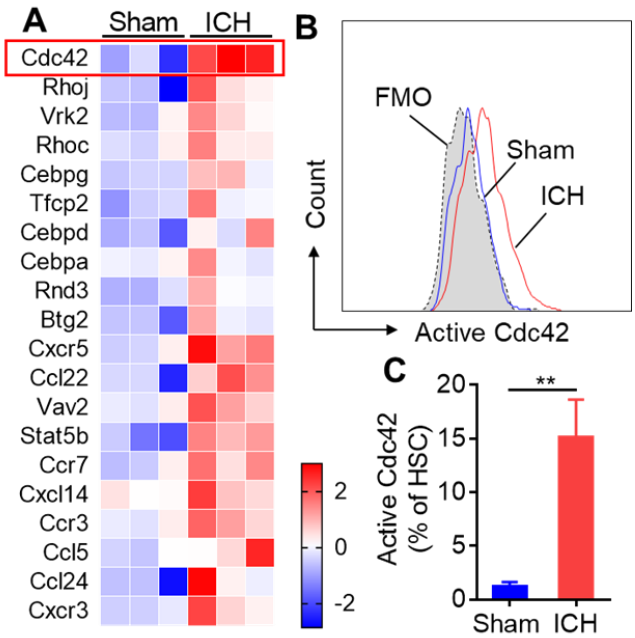

Figure 19. ICH induces a profound transcriptome change of HSCs.

ICH was induced by collagenase injection in 3-months old male C57BL/6J mice. Bone marrow was obtained from the femoral bone of ICH or sham mice 3 days after surgery. HSCs ($Lin^-Sca\text{-}1^+c\text{-}kit^+CD34^-Flk2^-CD48^-CD150^+$) were sorted by flow cytometry and mRNAs were extracted for unbiased profiling by Nanostring. (**A**) Heat map show altered genes relating to myeloid differentiation as well as cytokines/chemokines receptors in HSCs from ICH vs. sham mice. n = 3 per group. (**B-C**) Expression of active Cdc42 (GTP-bound form) in HSCs from indicated groups of mice assessed by flow cytometry. n = 4 per group. Mean ± SEM. $^{**}P < 0.01$.

Blockade of Cdc42 abolished ICH-induced increase of monocyte hematopoiesis in bone marrow and exacerbates ICH injury.

Rho GTPase Cdc42 regulates the adhesion, migration, homing, and cell cycle progression of HSCs. In HSCs, Cdc42 has been reported as a key regulator for tilting differentiation towards myeloid production[115-117]. Transcriptome sequencing of HSCs here, displayed the significant

upregulation of Cdc42 and other GTPase molecules in the HSCs of ICH mice. Therefore, I investigated whether Cdc42 acts as a molecular switch within HSCs to mediate the ICH-induced hemopoietic change. To this end, a selective Cdc42 inhibitor CASIN was used as a target modulator. Upon treatment with CASIN, the number of HSCs in bone marrow were decreased by approximately three-fold in mice at day 3, reduction in HSC proliferation activity was also evident (**Figure 20A**). Correspondingly, the variety of myeloid progenitors were also reduced upon CASIN treatment (**Figure 20B**); notably, the production of Ly6C^{low} monocytes was inhibited in CASIN treated ICH mice, monocyte expression of anti-inflammatory cytokine IL-10 was also reduced (**Figure 20C**).

For brain infiltrating immune cells following ICH, CASIN treatment decreased anti-inflammatory monocytes in the brain by about three-fold at day 3 after ICH compared to control mice (**Figure 21A**). IL-10-producing macrophages are similarly reduced by CASIN treatment in the ICH group (**Figure 21B**). In addition, the alternative activation markers of macrophages in the brain are also decreased in treated mice (**Figure 21C-D**). Relative to control mice, neurological deficits evaluated by mNSS was exacerbated at days 4 and 7 in ICH mice treated with CASIN (**Figure 21E**), sensorimotor function recovery measured by cylinder test was also abrogated upon CASIN treatment at days 4 and 7 after ICH (**Figure 21F**). Measurement of the hematoma volume at day 7 revealed that hematoma clearance was arrested by CASIN treatment (**Figure 21G**). These outcomes suggest that Cdc42 mediates the myeloid-inclined hematopoiesis in bone marrow HSCs after ICH, which may contribute to the hematoma clearance and functional recovery of ICH.

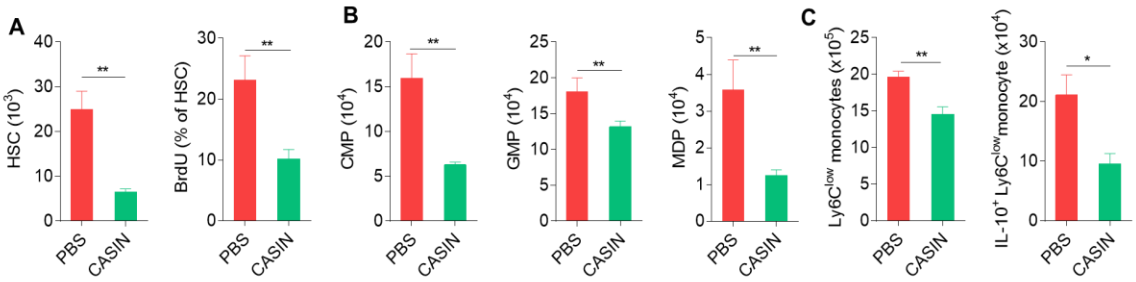

Figure 20. Cdc42 inhibition abolishes ICH-induced increase of monocyte hematopoiesis in bone marrow.

ICH was induced by collagenase injection in 3 month old male C57BL/6J mice, a Cdc42 inhibitor CASIN was given intraperitoneally immediately after ICH induction at a dosage of 2 mg/kg, repeated every 2 days. Bone marrow was obtained from femoral bones of ICH or sham mice 3 days after surgery. Flow cytometry was conducted to evaluate the bone marrow response. (**A**) HSC number and incorporation of BrdU at day 3 after ICH. (**B**) Cell counts of myeloid progenitors at day 3 after ICH. (**C**) Ly6C^{low} monocytes and IL-10-producing Ly6C^{low} monocyte counts in bone marrow of at day 3 after ICH. n = 8 per group. Mean ± SEM. **P* < 0.05, ***P* < 0.01.

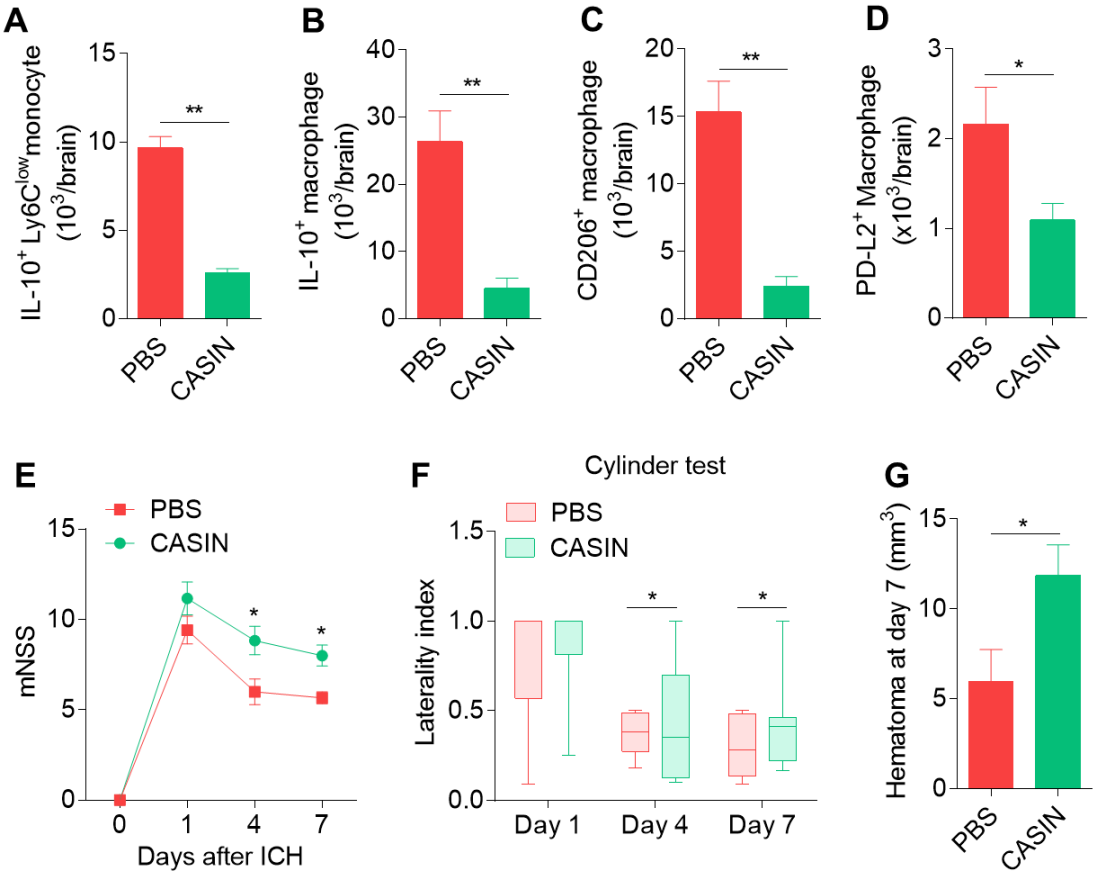

Figure 21. Cdc42 inhibition reduces Ly6^{low} monocytes in the ICH brain and exacerbated ICH injury.

ICH was induced by collagenase injection in 3 month old male C57BL/6J mice, a Cdc42 inhibitor CASIN was given intraperitoneally immediately after ICH induction at a dosage of 2 mg/kg, repeated every 2 days. (**A**) IL-10 producing monocyte counts in the brain at day 3 after ICH, n = 8 per group. (**B**) IL-10 producing macrophages and alternative activated CD206^{+} (**C**), PD-L2^{+}(**D**) macrophages counts in the brain at day 3 after ICH, n = 8 per group. (**E**) mNSS score from baseline to day 7 after ICH n = 12 per group, (**F**) Sensorimotor function evaluated by cylinder test at indicated time points after ICH, box indicates median and interquartile range, whiskers indicate 5-95 percentile. n = 12 per group. (**G**) Hematoma volume at day 7, n = 12 per group. In **A-E** and **G**, Mean ± SEM. *P < 0.05, **P < 0.01.

β3 agonist mirabegron enhances ICH-induced production of Ly6C^{low} monocytes and hematoma clearance.

Next, I sought to investigate whether promoting anti-inflammatory monocyte hematopoiesis could accelerate hematoma clearance and improve disease outcome of ICH. Mirabegron is a selective β3-adrenergic receptor agonist that has been approved for the treatment of overactive bladder[118, 119]. After demonstrating that increased sympathetic nervous system activity mediated Ly6C^{low} monocyte hematopoiesis after ICH, I tested whether oral administration of mirabegron was able to enhance monocyte production and improve ICH outcome. Mirabegron was administered to mice after ICH at a dose of 2 mg/kg daily, a dosage equal to the clinical treatment in overactive bladder[118]. HSC number in the bone marrow was increased by approximately 50% in mice treated at day 3 post-ICH compared to controls (**Figure 22A**); myeloid progenitors were also increased upon treatment in a similar trend (**Figure 22B**). With regard to monocytes production, total Ly6C^{low} monocytes and Ly6C^{low} monocytes in bone marrow were increased by a factor in mirabegron treated ICH mice (**Figure 22C**). These results indicate that mirabegron treatment was effectual in promoting Ly6C^{low} monocyte production in bone marrow after ICH.

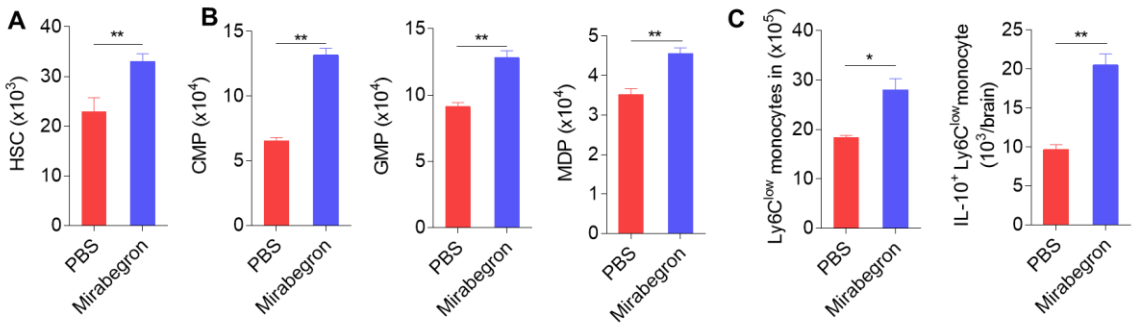

Figure 22. An Adrenergic β3 receptor agonist enhances bone marrow production of IL-10-producing Ly6C^{low} monocytes after ICH.

ICH was induced by collagenase injection in 3 month old male C57BL/6J mice, a selective β3 receptor agonist mirabegron was given to mice immediately after ICH induction at a dose of 2 mg/kg via oral gavage daily. Bone marrow was obtained at day 3 after ICH. (**A**) HSC number in bone marrow at day 3 after ICH. (**B**) Cell counts of myeloid progenitors in bone marrow at day 3 after ICH. (**C**) Ly6C^{low} monocytes and Il-10 producing Ly6C^{low} monocyte counts in bone marrow of at day 3 after ICH. n = 8 per group. Mean ± SEM. *P < 0.05, **P < 0.01.

Whether the increased monocytes production in bone marrow by mirabegron could impact the immune environment in the brain of ICH mice was the next question to examine. Flow cytometric analysis revealed that mirabegron increased IL-10$^+$ anti-inflammatory monocytes and derivative macrophages by approximately 50% in the brain at day 3 after ICH compared to mice treated with PBS vehicle (**Figure 23A-B**). In addition, alternatively activated macrophages in the brain were also significantly increased by mirabegron treatment (**Figure 23B**). Interestingly, brain-infiltrating neutrophils and lymphocytes were both reduced in mice treated with mirabegron at day 3 after ICH (**Figure 23C**). This indicates that mirabegron increases the accumulation of anti-inflammatory monocytes to the brain and reduces brain inflammation after ICH. Given this insight whether mirabegron could accelerate hematoma absorption and promote functional recovery in ICH mice becomes a central question. A series of established motor-sensory tests in addition to injury indicators were used to evaluate recovery in ICH mice. While there was no significant

difference regarding neurodeficits measured by mNSS and sensorimotor function, evaluated by cylinder test at day 1 after ICH between groups, mice treated with mirabegron showed significant reduction in neurodeficits at days 4 and 7 after ICH relative to control mice, as well as improved sensorimotor function (**Figure 23D-E**). Notably, mirabegron treated mice had reduced hematoma volumes at day 7 compared to vehicle treated group (**Figure 23F**). In all, these data demonstrate that β3-adrenergic receptor activation via mirabegron reduced brain inflammation, promoted hematoma clearance, and improved neurological recovery of ICH mice.

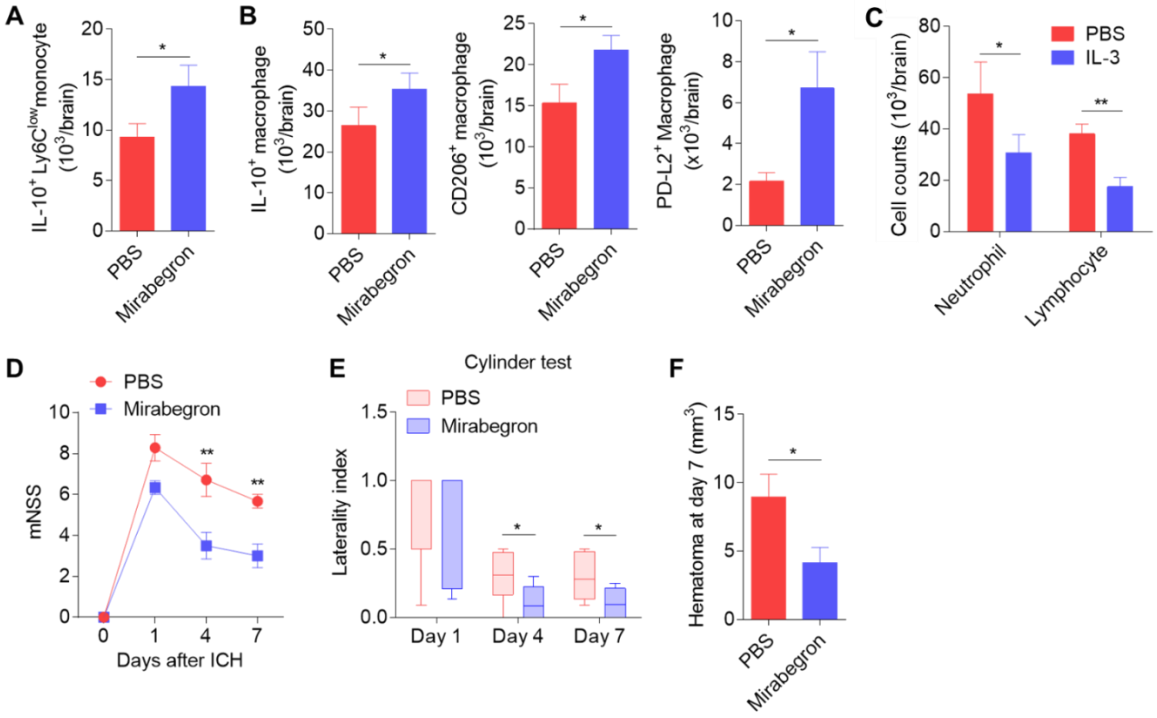

Figure 23. Adrenergic β3 receptor activation reduces brain inflammation and improved hematoma clearance.

ICH was induced by collagenase injection in 3 month old male C57BL/6J mice, a selective β3 receptor agonist mirabegron was given to mice immediately after ICH induction at a dose of 2 mg/kg via oral gavage daily. Brain tissue was obtained at day 3 for flow cytometry detection of immune cells in the brain. (**A**) IL-10-producing Ly6C^{low} monocytes in the brain at day 3 post-ICH. (**B**) IL-10^{+} macrophages and alternatively activated macrophages (CD206^{+} and PD-L2^{+}) in the

brain at day 3 post-ICH. (**C**) Counts of brain-infiltrating neutrophils and lymphocytes in ICH mice receiving PBS or IL-3. (**D**) Neurological deficits measured via mNSS from baseline to day 7 after ICH. (**E**) Sensorimotor function evaluated by cylinder test at indicated time points, box indicates median and interquartile range, whiskers indicate 5-95 percentile. (**F**) Hematoma volume at day 7. n = 8 per group in **A-C**, n = 12 per group in **D-F**. Mean ± s.e.m. **P* < 0.05, ***P* < 0.01.

IL-3 treatment accelerates hematoma clearance and functional recovery after ICH

Upon identifying that Cdc42 is a key molecule within HSCs which mediates the hemopoietic response to ICH, I sought to investigate whether pharmacological activation of Cdc42 could expand the generation of anti-inflammatory monocytes and improve ICH outcome. IL-3 is a known hematopoietic growth factor capable of activating endogenous Rac-1, Rac-2, and Cdc42[120]. Therefore, I tested whether recombinant IL-3 treatment could leverage the production of Ly6C^{low} monocytes and beneficially impact ICH outcome in our mouse model. Similar to mirabegron, IL-3 treatment increased HSCs in the bone marrow by approximately 50% at day 3 after ICH (**Figure 24A**), additionally, myeloid progenitors GMP and MDP counts were also increased in bone marrow in treated mice (**Figure 24B**). As for monocytes, the production of Ly6C^{low} monocytes and anti-inflammatory macrophages were also increased at day 3 after ICH in mice treated with IL-3 (**Figure 24C**).

The counts of Ly6C^{low} monocytes and macrophages were significantly increased at day 3 after ICH in mice receiving IL-3 versus PBS control (**Figure 25A-B**). Macrophages in the brain of ICH mice receiving IL-3 displayed upregulation of alternative activation markers CD206 and PD-L2 (**Figure 25B**). Furthermore, the infiltration of neutrophils and lymphocytes was inhibited by IL-3 treatment (**Figure 25C**). Compared to PBS controls, IL-3-treated mice had significant reductions in neurological deficit measured by mNSS from day 1 to day 7 after ICH (**Figure 25D**). Additionally, IL-3 promoted sensorimotor function recovery at days 4 and 7 following ICH (**Figure 25E**). The reduced hematoma volume in ICH mice receiving IL-3 suggests accelerated hematoma clearance (**Figure 25F**).

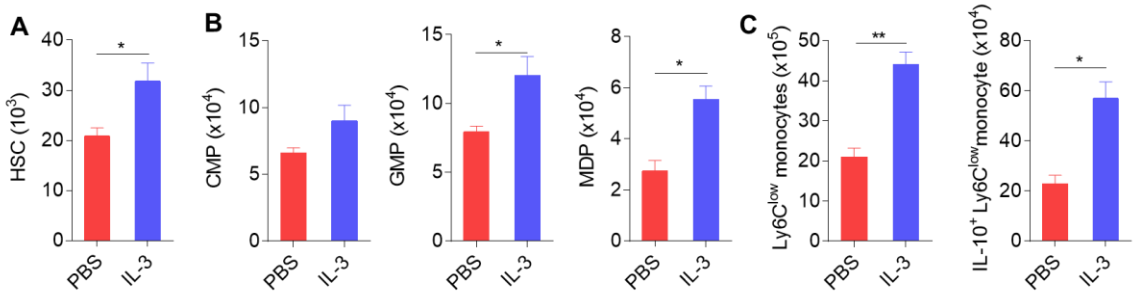

Figure 24. IL-3 treatment enhances ICH-induced hematopoiesis of Ly6C^{low} monocytes in the bone marrow.

ICH was induced by collagenase injection in 3 month old male C57BL/6J mice, recombinant IL-3 was given to ICH mice immediately after model induction via intraperitoneal injection at a dose of 600ng daily. Bone marrow was obtained at day 3 after ICH for flow cytometry detection. (**A**) HSC number in bone marrow. (**B**) Cell counts of myeloid progenitors in bone marrow at day 3 after ICH. (**C**) Ly6C^{low} monocytes and Il-10 producing Ly6C^{low} monocyte counts in bone marrow of at day 3 after ICH. n = 8 per group. Mean ± SEM. **P* < 0.05, ***P* < 0.01.

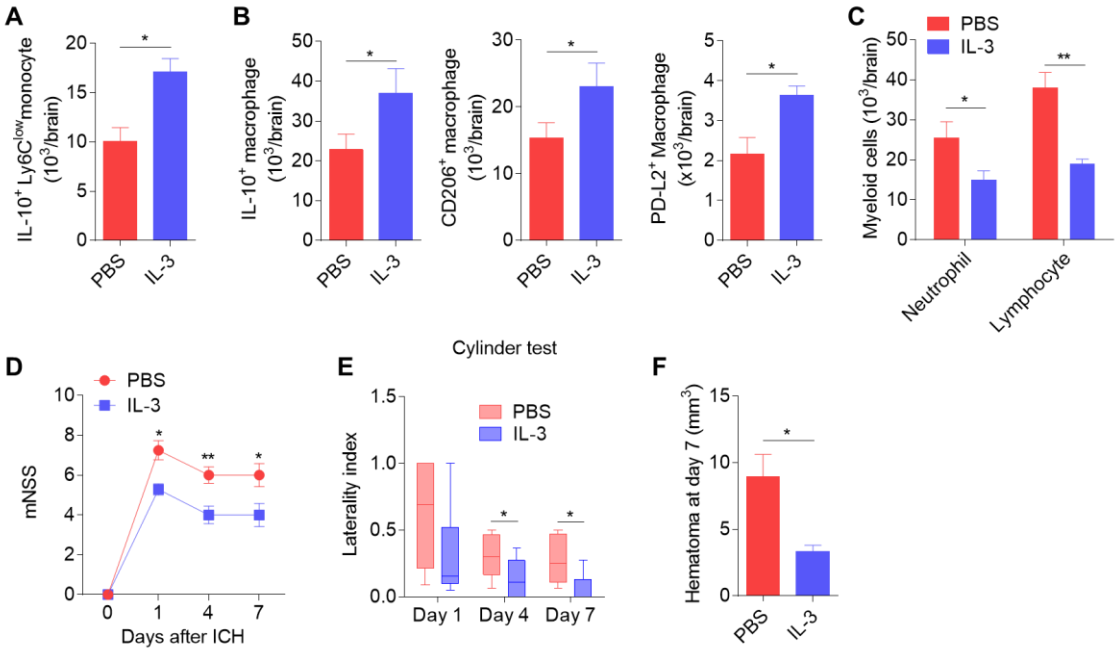

Figure 25. IL-3 treatment reduces brain inflammation and promoted hematoma clearance after ICH.

ICH was induced by collagenase injection in 3 month old male C57BL/6J mice, recombinant IL-3 was given to ICH mice immediately after ICH induction via intraperitoneal injection at a dose of 600 ng daily. Brain tissue was obtained at day 3 for flow cytometry detection of immune cells in the brain. (**A**) IL-10-producing Ly6C^{low} monocytes in the brain at day 3 post-ICH. (**B**) IL-10^{+} macrophages and alternatively activated macrophages (CD206^{+} and PD-L2^{+}) in the brain at day 3 post-ICH. (**C**) Brain infiltrating neutrophils and lymphocytes counts in the brain at day 3 after ICH. (D) Neurological deficits measured via mNSS from baseline to day 7 after ICH. (**E**) Sensorimotor function evaluated by cylinder test at indicated time points, box indicates median and interquartile range, whiskers indicate 5-95 percentile. (**F**) Hematoma volume at day 7. In **A-C**, n = 8 per group. In **D-F**, n = 12 per group. Mean ± SEM. *P < 0.05, **P < 0.01.

Summary

- ICH swiftly skews bone marrow HSCs towards the myeloid lineage.
- Lineage tracing reveals a predominantly augmented hematopoiesis of Ly6C^{low} monocytes that home to the ICH brain.
- Newly produced bone marrow Ly6C^{low} monocytes generate alternatively activated macrophages and suppress neuroinflammation in the ICH brain.
- ICH promotes bone marrow hematopoiesis of Ly6C^{low} monocytes via β3-adrenergic innervation and Cdc42.
- Stimulation of β3-adrenergic receptor promotes bone marrow hematopoiesis of Ly6C^{low} monocytes and suppresses neuroinflammation after ICH.

CHAPTER 6

DISCUSSION

Here, I systemically investigated the focal and peripheral immune responses in the setting of ICH. First, in the perihematomal region within the brain after ICH, I identify that IL-15, which is highly expressed by astrocytes after ICH in patients and mouse models, expanded microglial response in the perihematomal region and skewed microglia towards a pro-inflammatory phenotype, manifested by increased expression of CD86, IL-1β, and TNF-α. This augmented microglial response exacerbated hemorrhagic brain injury and worsened ICH outcome in the animal model. These findings uncovered that IL-15 bridges the crosstalk between astrocytes and microglia in the setting of ICH, which drives the tissue damage and worsen outcome. Second, in the periphery, data reveals that increased sympathetic tone post-ICH activates the hematopoiesis system and skews the lineage commitment of HSCs towards a myeloid bias with increased production of $Ly6C^{low}$ monocytes. These new generated $Ly6C^{low}$ monocytes highly express anti-inflammatory cytokine IL-10, and efficiently migrate to the injured brain, giving rise to alternatively activated macrophages. These anti-inflammatory monocytes/macrophages reduce brain inflammation, promote hematoma clearance, and improve functional recovery in our animal model of ICH. In sum, these results deepen our understanding of the systemic immune response of an acute brain injury to the hematopoietic system. The panoramic deciphering of the focal and peripheral immune responses post-ICH paves the way in developing new therapeutic strategies to control acute brain injury and promote functional recovery after an ICH.

IL-15 bridges the crosstalk between astrocytes and microglia after ICH

The findings reported in the focal context of ICH immune response assigns a role to IL-15 as a mediator of astrocyte-microglia crosstalk in ICH (**Figure 26**). Accounting for over 50% of the brain cell mass, astrocytes weave their processes throughout the CNS, harboring delicate interactions with microglia[121, 122]. Following brain insults, astrocytes react robustly by releasing pro-inflammatory mediators that direct microglial activity and shape diverse neuropathologies[121, 122].

Together with an upregulation of CD86 and TNF-α, increased accumulation, enlarged cell bodies and diminished processes of microglia in the perihematomal tissue indicate enhanced pro-inflammatory activation of microglia in GFAP-IL-15^{tg} mice. In addition to the production of pro-inflammatory factors, microglia also possess diverse capacities of phagocytosis, antigen presentation, and secretion of anti-inflammatory factors[121]. These varied capabilities of microglia enables them to participate in hematoma clearance and resolution of tissue inflammation, depending on the timing and environment[59, 60]. Although the data here implicates astrocytic IL-15 as a driver of the pro-inflammatory response of microglia, whether and to what extent astrocytic IL-15 affects microglial impact on hematoma clearance and tissue repair are of interest and warrants further investigation. Together, these findings provide new evidence that astrocyte-derived IL-15 augments the pro-inflammatory response of microglia after ICH. These insights expand our knowledge of astrocyte-microglia crosstalk in CNS injury.

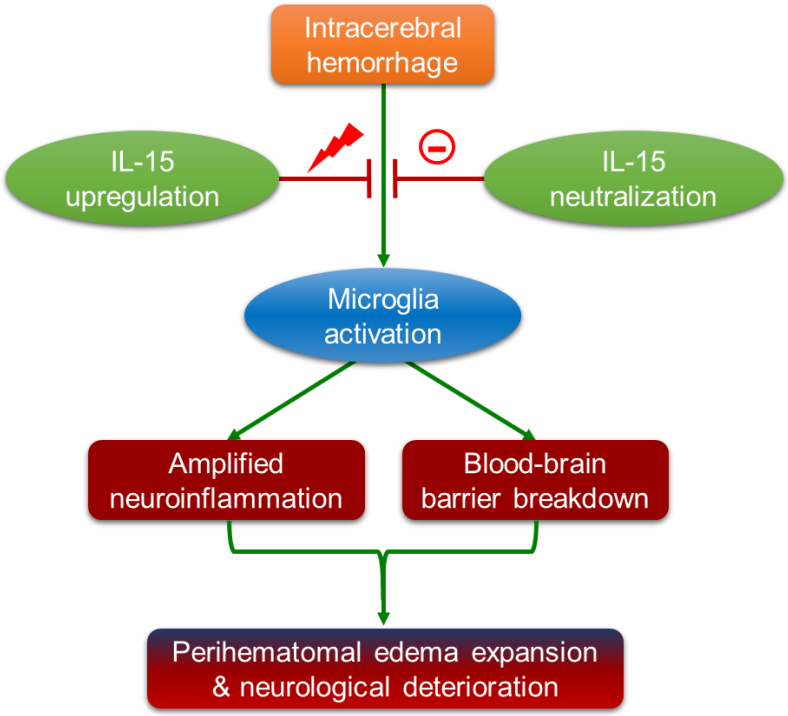

Figure 26. IL-15 bridges astrocyte-microglia crosstalk and exacerbates brain injury following ICH.

ICH induces upregulation of astrocytic IL-15 that shifts microglia toward pro-inflammatory response, leading to the expansion of PHE and deterioration of neurological outcome.

It is noteworthy that astrocyte-targeted expression of IL-15 had no significant impact on the numbers of brain-infiltrating immune cells, including T and B lymphocytes, monocytes, and neutrophils. However, the potential impact of these cells on astrocytic IL-15-induced exacerbation of ICH injury cannot be excluded. Although not addressed in this study, IL-15 could also participate in other aspects of neuroinflammation, given its chemotactic and pro-survival effects on peripheral immune cells such as $CD8^+$ T cells[93, 123, 124]. In addition, as the immune and inflammatory response harbors both beneficial and deleterious functions after ICH, future studies should be extended to examine the effects of IL-15 on the long-term neurological outcomes and tissue repair following ICH.

The present findings have clinical implications for targeting astrocytes, which are a prominent contributor to CNS inflammatory responses after ICH. In support of the translational relevance of this study, histological results show an increased concentration of $IL\text{-}15^+$ astrocytes in close proximity with microglia after ICH. Recent experimental studies have demonstrated immune interventions targeting key inflammatory mediators as a viable approach in restricting brain inflammation and tissue damage after ICH[27, 30]. Immune therapies targeting IL-1 are ongoing in an ICH clinical trial (NCT03737344), and promising results have been reported in patients with subarachnoid hemorrhage[125]. Therefore, the identification of astrocyte-derived IL-15 as a prominent contributor to ICH injury may facilitate future design of selective treatment for ICH patients.

Thus, our findings suggest IL-15 as an astrocyte-derived factor with prominent effects on ICH injury. As an increase of IL-15-expressing astrocytes is evident in the brain of ICH patients, further investigation is warranted to reveal the therapeutic potential of IL-15-modifying treatments in ICH.

ICH induces anti-inflammatory Ly6C^{low} monocyte hemopoiesis that benefit stroke outcome

Blood monocyte counts on admission are associated with neurological outcome in ICH patients[126-129], potentially due to neural damage and pro-inflammatory effects by classical Ly6C^{hi} monocytes[78, 130]. Our group has previously discovered that ICH patients underwent lymphopenia after disease onset persists for up to 2 weeks, however, CD11b^{+} myeloid cells showed an increasing trend on the contrary[4]. Given to the rapid turnover of myeloid cells in the circulation, the sustained increase requires replenishment from the hematopoietic system or extra-medullar reservoirs. The spleen is the biggest peripheral reservoir of monocytes and responds to systemic stimulus, such as infection, with rapid changes in gross volume. However, ICH induces significant spleen atrophy during the acute and subacute phases[4], which dampens the possibility that the spleen sustains the myeloid cells supply after ICH. In this dissertation, I identify that increased adrenergic activity after ICH induces the proliferation of the most up-stream long-term HSCs, leading to increased numbers of myeloid progenitors in the bone marrow. The newly generated monocytes are primarily Ly6C^{low} patrolling monocytes but not neutrophils or Ly6C^{hi} monocytes. These nascent Ly6C^{low} patrolling monocytes possess an anti-inflammatory profile and give rise to alternatively activated macrophages in the injured brain (**Figure 27**). While Ly6C^{hi} monocytes are known as pro-inflammatory cells and contribute to tissue damage, Ly6C^{low} patrolling monocytes and alternatively activated macrophages promote inflammation resolution and wound repair[113]. Therefore, these findings suggest that circulating Ly6C^{hi} monocytes are first mobilized to the brain after ICH and contribute to secondary brain injury, with the activation of bone marrow hematopoiesis of Ly6C^{low} patrolling monocytes as well as the quick turnover of Ly6C^{hi} monocytes, Ly6C^{low} monocytes then (likely after day 3) take over as the main monocyte subtype in the brain, which give rise to alternatively activated macrophages, resolving brain inflammation and promoting tissue repair. It has been reported that spleen monocytes exerts more rigorous pro-inflammatory profile than bone marrow monocytes[110], in this regard, the spleen atrophy post-ICH may partially contribute to the enhanced anti-inflammatory monocyte generation.

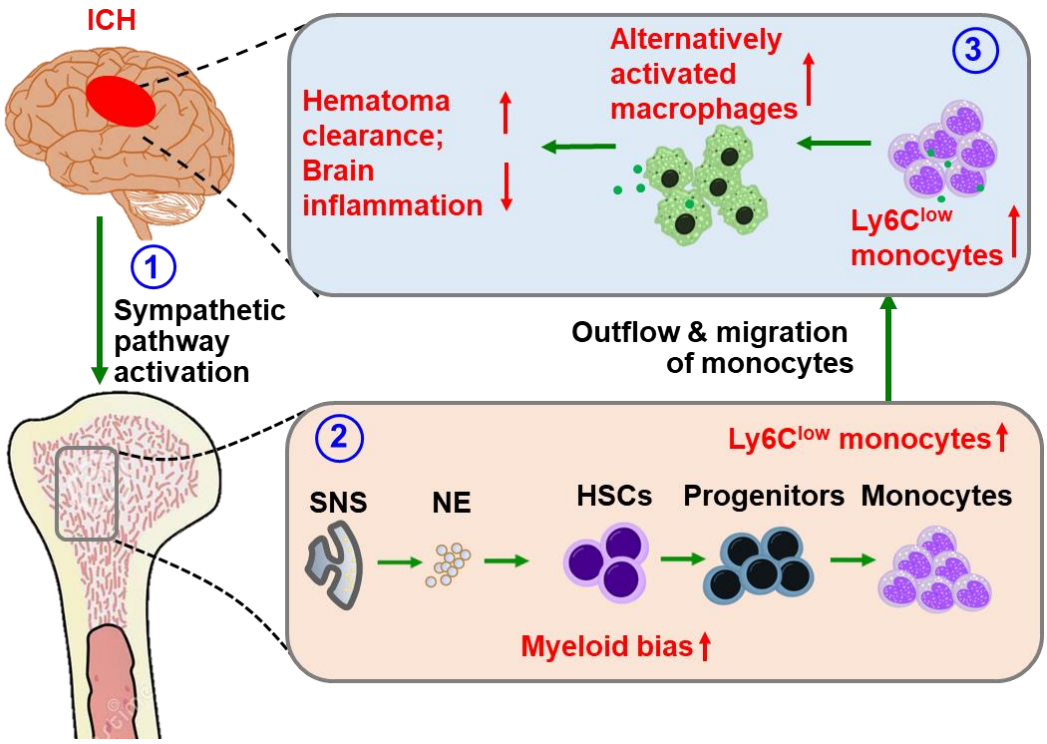

Figure 27. ICH induces bone marrow hematopoiesis of Ly6C^{low} monocytes that reduce brain inflammation and accelerate hematoma clearance.

(**1**) ICH activates the sympathetic pathway mediated by norepinephrine (NE). (**2**) Increased adrenergic input activate quiescent HSCs in bone marrow, giving rising to a biased generation of myeloid progenitors and increased outflow of anti-inflammatory Ly6C^{low} monocytes. (**3**) Ly6C^{low} monocytes home to the brain and give rise to alternatively activated macrophages that accelerate hematoma clearance and resolution of brain inflammation, leading to improved ICH outcome.

The identification of the beneficial effects of hematogenous Ly6C^{low} monocytes in conjunction with the mechanisms underlying the response, prompts the opportunity to leverage anti-inflammatory monocytes generation in improving ICH outcome. One of the plausible strategies explored is to enhance β3-adrenergic receptor signaling by mirabegron, which is a selective β3 agonist approved by FDA for the treatment of overactive bladder. A clinically derived dosage of mirabegron treatment significantly promoted Ly6C^{low} patrolling monocytes production in ICH mice, which promoted hematoma clearance and stroke recovery. This discovery is of great

clinical translational value given the apparent safety of mirabegron in clinical use. The findings of HSC endogenous Cdc42 activation serve as another therapeutic target for promoting anti-inflammatory monocyte generation. Besides neurogenic signals, hematopoietic activities are closely regulated by cytokines. For instance, IL-3 is a hematopoietic growth factor which readily activates Cdc42. Treatment with recombinant IL-3 showed similar effects on $Ly6C^{low}$ monocytes generation and stroke outcome in ICH mice, as observed with mirabegron treatment. The remaining question is whether these new generated monocytes can promote tissue remodeling and affect long-term benefits. Additionally, given that stroke patients are often complicated with vascular changes like atherosclerosis, and monocytes play a key role in plaque stability, the impacts of mirabegron and IL-3 on atherosclerosis progression is noted for future study.

From the concept that brain is an immune-privileged organ to the recognition of increasing complexity of interactions between nervous system and peripheral organs, our understanding of neuroimmune interaction has evolved considerably. In the setting of acute brain injury, it has been recognized that brain injury impacts the immune responses in peripheral tissues including liver, spleen, heart, intestine, and circulation. This dissertation reveals that acute brain injury swiftly activates the hematopoietic system, advancing our understanding of immune activation outside the brain in response to acute brain insults.

CONCLUSION AND FUTURE PERSPECTIVES

In all, this study unveils the intimate crosstalk between the immune and nervous systems within and outside the brain in response to acute brain insults. The identified neural-immune interactions possess organ-specific features that differ among individual organ systems and are mediated by distinct types of immune cells and factors. Our increasing understanding on this topic is expected to provide insights into the initiation, progression, and resolution of neuroinflammation and identify novel treatment options that might facilitate the future design of immunomodulatory therapies to benefit patients with acute brain injury.

Immune responses after acute brain injury involve multiple cells, molecules, and organs, and take place across these different levels. Here, the scope of investigation is limited to glial cells interaction in the brain as well as bone marrow responses in periphery. A comprehensive understanding of the immune responses after hemorrhagic brain injury will require a panoramic pursuit of the immune processes across different organs and at the systems levels. In addition, the application of new state-of-art and multi-omics approaches like single cell sequencing, mass spectrometry will accelerate our investigations in the future and promote the discovery of new insights that could be valuable for the translations of pre-clinical findings to clinical practice.

The reporting that glial cell interaction post-ICH promotes the development of neuroinflammation which exacerbates hemorrhagic brain injury prompts the question of what triggers the upregulation of IL-15 in astrocytes, and more broadly if there are any key genes/molecules that critically switch focal brain inflammation on after ICH. If such a “switch” exists, the identification of it could present a therapeutic target to improve ICH outcome via immune modulation.

By adopting FDG-PET imaging, I show that ICH induced a significant upregulation of cellular activity in the spinal column in live mice. Due to the imaging limitations, I was unable to show the bone marrow activity in whole body bones like femur, tibia, and the skull. Though it is clearly shown that femur bone marrow responses increased via flow cytometry; an unanswered

question is whether the bone marrow responses differ in different marrow niches of the body. For example, since the skull is the closest bone proximal to the brain, and a recent study shows that myeloid cells in the skull bone marrow are actively recruited to migrate to the brain parenchyma after ischemia through microvessels between the bone surface and brain cortex, does the skull bone marrow respond differently from peripheral bones like femur that I mainly studied in this study, is an interesting point to investigate in the future.

This study has several limitations. First, this study only deals with two examples of many players involved in focal and systemic effects of ICH, i.e. IL-15 and HSCs. This is in part due to limited time and resources during my PhD work. Other key elements of immune system after ICH such as meningeal lymphatic vessels deserve further investigation in future studies. Second, limited approaches were used to study focal and systemic immune response after ICH. This study could be strengthened by incorporation of several novel technologies, including single-cell sequencing, two-photon *in vivo* imaging and 3D MRI imaging, etc. Results from these approaches could illustrate a broad landscape that is more useful for clinical translation. Third, there are several questions remain to be answered. Forth, given the discrepancy between animal models and ICH patients, caveats should be taken when interpret our results in experimental ICH models in relation to ICH patients. Finally, there is a dichotomy of brain's focal and systemic immune response upon the occurrence of ICH. Therefore, a better understanding of the kinetics or potentially differential effects of focal versus systemic immune response in ICH outcome would offer novel insight into how to modulate these two compartments to achieve better outcome for ICH patients.

The paramount question is whether a greater understanding of brain and systemic immune responses after ICH can lead to successful clinical translation of immune modulation as a therapeutic approach to ICH. Recent completed pilot clinical trials of an immune modulator, fingolimod, in stroke patients suggest that immune modulation could be a potential approach to limit acute brain injury. Moreover, two international clinical trials evaluated the efficacy of

natalizumab, a monoclonal antibody (mAb) that prevents the trafficking of leukocytes across the BBB, in ischemic stroke (ACTION I: NCT01955707; ACTION II: NCT02730455). Although the results in these two trials did not show clear-cut benefit of natalizumab on functional outcome in stroke patients, these efforts highlight the renewed interests of immune interventions in stroke. Notably, a randomized, placebo-controlled, and double blinded trial of BAF312 in ongoing in ICH patients (NCT03338998). BAF312 is a sphingosine 1-phosphate receptor modulator that could potentially limit brain inflammation after ICH. Results from this trial may provide novel and more conclusive information on the potential benefit of curbing neuroinflammation in ICH. Additionally, in a large randomized multi-central study, 10,016 patients with previous myocardial infarction and a high-sensitivity C-reactive protein level, demonstrated that canakinumab, a therapeutic monoclonal antibody targeting IL-1β, led to a significantly lower rate of recurrent cardiovascular events than placebo, independent of lipid-level lowering. This study convincingly indicates that systemic inflammation may be responsible for recurrent cardiovascular events and that immune inhibition of an innate immune pathway is sufficient to reduce the risks. Therefore, I believe that a better understanding of the focal brain inflammation as well as peripheral immune responses will potentially offer insight on how to manage these compartments to improve patients' outcome.

As brain inflammation following ICH involves in both in situ DAMP-activated microglia coordinated events, as well as homing of peripheral immune cells. In the peripheral compartments, the adoption of multiple medications interfering in cell migration, proliferation, or depleting cells are employed for the management of patients with multiple sclerosis. Emerging therapies targeting microglia (CFSR1) or astrocytes (miglustat) may offer new avenue to curb brain inflammation within the brain. Indeed, preclinical studies in ICH and EAE models have shown that these two approaches reduce brain immune reactions and subsequent neurological deficit[104, 131]. Therefore, I propose that effective and timely reducing brain inflammation can be achieved by combination approaches acting on both peripheral and CNS compartments (**Figure 28**). This may lead to the long sought after measurable clinical benefits for patients with ICH, and other type of brain injuries.

Finally, the progress of the field of stroke immunology is ultimately dependent on whether such studies, as the one here, can offer new therapeutic options by deepening the understanding of emergence and progression of brain inflammation. Due to the complex pathophysiological processes involved, there are a number of key outstanding questions needs to be resolved regarding the dynamic and resolution of inflammation and its relation to patient outcome and recovery (**Table 2**); it is my belief that only when we have an improved understanding of these questions can substantial milestones be reached in crossing the chasm between preclinical findings and patient improvement.

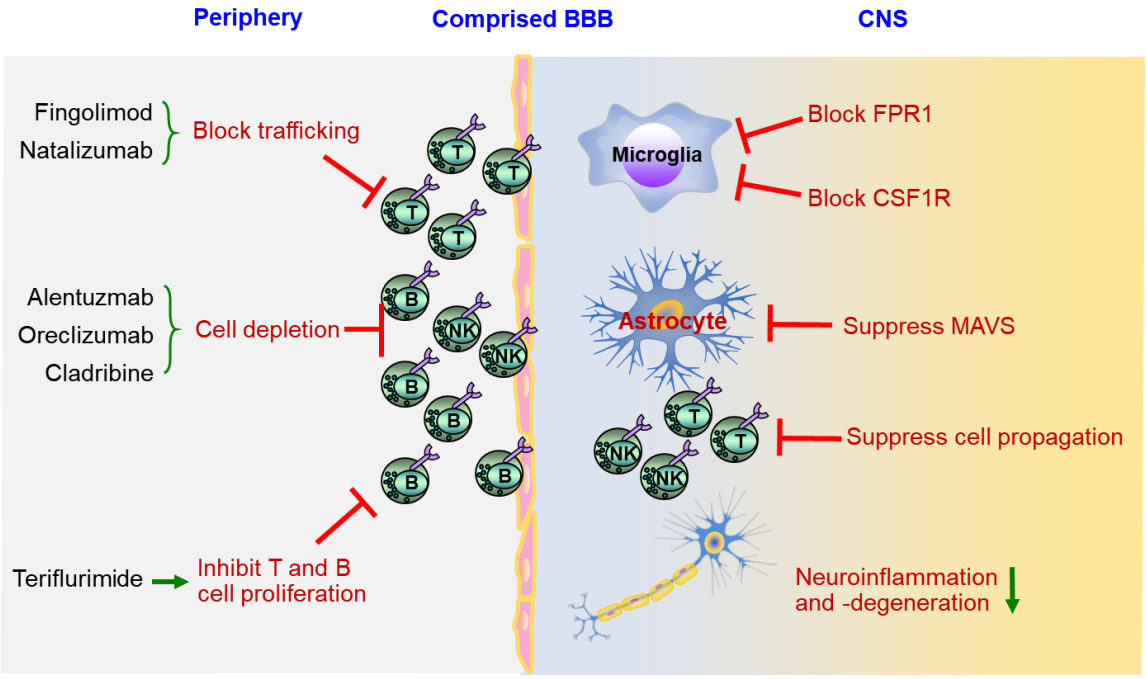

Figure 28. Peripheral and CNS approaches to control ICH triggered neuroinflammation and neurodegeneration.

Table 2. Outstanding questions in ICH immunology

● Is there a master switch for neuroinflammation following ICH? If so, is it druggable? ● What is the nature of interactions between peripherally arrived immune cells and microglia or astrocytes? ● What are the roles of immune response in tissue remodeling, focal vs. global brain inflammation, and autoimmunity after ICH? ● Regarding clinical trials, how to choose time window (when, frequency and duration), immune modulatory modalities (single or multiple cells /proteins) for immune intervention after ICH? ● What type of ICH patients will be better responders for immune intervention:

REFERENCES

1. Shi K, Tian DC, Li ZG, Ducruet AF, Lawton MT, Shi FD. Global brain inflammation in stroke. *Lancet Neurol*. 2019

2. Chamorro A, Meisel A, Planas AM, Urra X, van de Beek D, Veltkamp R. The immunology of acute stroke. *Nat Rev Neurol*. 2012;8:401-410

3. Urday S, Kimberly WT, Beslow LA, Vortmeyer AO, Selim MH, Rosand J, Simard JM, Sheth KN. Targeting secondary injury in intracerebral haemorrhage--perihaematomal oedema. *Nat Rev Neurol*. 2015;11:111-122

4. Zhang J, Shi K, Li Z, Li M, Han Y, Wang L, Zhang Z, Yu C, Zhang F, Song L, Dong JF, La Cava A, Sheth KN, Shi FD. Organ- and cell-specific immune responses are associated with the outcomes of intracerebral hemorrhage. *FASEB J*. 2018;32:220-229

5. Liu Q, Jin WN, Liu Y, Shi K, Sun H, Zhang F, Zhang C, Gonzales RJ, Sheth KN, La Cava A, Shi FD. Brain ischemia suppresses immunity in the periphery and brain via different neurogenic innervations. *Immunity*. 2017;46:474-487

6. Shi K, Wood K, Shi FD, Wang X, Liu Q. Stroke-induced immunosuppression and poststroke infection. *Stroke Vasc Neurol*. 2018;3:34-41

7. Meisel C, Schwab JM, Prass K, Meisel A, Dirnagl U. Central nervous system injury-induced immune deficiency syndrome. *Nat Rev Neurosci*. 2005;6:775-786

8. Keep RF, Hua Y, Xi G. Intracerebral haemorrhage: Mechanisms of injury and therapeutic targets. *Lancet Neurol*. 2012;11:720-731

9. An SJ, Kim TJ, Yoon BW. Epidemiology, risk factors, and clinical features of intracerebral hemorrhage: An update. *Journal of stroke*. 2017;19:3-10

10. Caceres JA, Goldstein JN. Intracranial hemorrhage. *Emergency medicine clinics of North America*. 2012;30:771-794

11. Broderick J, Connolly S, Feldmann E, Hanley D, Kase C, Krieger D, Mayberg M, Morgenstern L, Ogilvy CS, Vespa P, Zuccarello M, American Heart A, American Stroke Association Stroke C, High Blood Pressure Research C, Quality of C, Outcomes in Research Interdisciplinary Working G. Guidelines for the management of spontaneous intracerebral hemorrhage in adults: 2007 update: A guideline from the american heart association/american stroke association stroke council, high blood pressure research

council, and the quality of care and outcomes in research interdisciplinary working group. *Stroke*. 2007;38:2001-2023

12. Zheng H, Chen C, Zhang J, Hu Z. Mechanism and therapy of brain edema after intracerebral hemorrhage. *Cerebrovascular diseases*. 2016;42:155-169

13. Selim M, Foster LD, Moy CS, Xi G, Hill MD, Morgenstern LB, Greenberg SM, James ML, Singh V, Clark WM, Norton C, Palesch YY, Yeatts SD, i DEFI. Deferoxamine mesylate in patients with intracerebral haemorrhage (i-def): A multicentre, randomised, placebo-controlled, double-blind phase 2 trial. *Lancet Neurol*. 2019;18:428-438

14. Xi G, Keep RF, Hoff JT. Mechanisms of brain injury after intracerebral haemorrhage. *Lancet Neurol*. 2006;5:53-63

15. Fisher CM. Pathological observations in hypertensive cerebral hemorrhage. *Journal of neuropathology and experimental neurology*. 1971;30:536-550

16. Lim-Hing K, Rincon F. Secondary hematoma expansion and perihemorrhagic edema after intracerebral hemorrhage: From bench work to practical aspects. *Front Neurol*. 2017;8:74

17. Mayer SA, Lignelli A, Fink ME, Kessler DB, Thomas CE, Swarup R, Van Heertum RL. Perilesional blood flow and edema formation in acute intracerebral hemorrhage: A spect study. *Stroke*. 1998;29:1791-1798

18. de Oliveira Manoel AL, Goffi A, Zampieri FG, Turkel-Parrella D, Duggal A, Marotta TR, Macdonald RL, Abrahamson S. The critical care management of spontaneous intracranial hemorrhage: A contemporary review. *Critical care*. 2016;20:272

19. Freeman WD, Brott TG, Barrett KM, Castillo PR, Deen HG, Jr., Czervionke LF, Meschia JF. Recombinant factor viia for rapid reversal of warfarin anticoagulation in acute intracranial hemorrhage. *Mayo Clinic proceedings*. 2004;79:1495-1500

20. Mayer SA, Brun NC, Broderick J, Davis S, Diringer MN, Skolnick BE, Steiner T, Europe/AustralAsia NovoSeven ICHTI. Safety and feasibility of recombinant factor viia for acute intracerebral hemorrhage. *Stroke*. 2005;36:74-79

21. Alvarez-Sabin J, Delgado P, Abilleira S, Molina CA, Arenillas J, Ribo M, Santamarina E, Quintana M, Monasterio J, Montaner J. Temporal profile of matrix metalloproteinases and their inhibitors after spontaneous intracerebral hemorrhage: Relationship to clinical and radiological outcome. *Stroke*. 2004;35:1316-1322

22. Xi G, Keep RF, Hoff JT. Erythrocytes and delayed brain edema formation following intracerebral hemorrhage in rats. *Journal of neurosurgery*. 1998;89:991-996

23. Xi G, Wagner KR, Keep RF, Hua Y, de Courten-Myers GM, Broderick JP, Brott TG, Hoff JT. Role of blood clot formation on early edema development after experimental intracerebral hemorrhage. *Stroke*. 1998;29:2580-2586

24. Urday S, Beslow LA, Goldstein DW, Vashkevich A, Ayres AM, Battey TW, Selim MH, Kimberly WT, Rosand J, Sheth KN. Measurement of perihematomal edema in intracerebral hemorrhage. *Stroke*. 2015;46:1116-1119

25. Murthy SB, Urday S, Beslow LA, Dawson J, Lees K, Kimberly WT, Iadecola C, Kamel H, Hanley DF, Sheth KN, Ziai WC, Collaborators VI. Rate of perihaematomal oedema expansion is associated with poor clinical outcomes in intracerebral haemorrhage. *Journal of neurology, neurosurgery, and psychiatry*. 2016;87:1169-1173

26. Urday S, Beslow LA, Dai F, Zhang F, Battey TW, Vashkevich A, Ayres AM, Leasure AC, Selim MH, Simard JM, Rosand J, Kimberly WT, Sheth KN. Rate of perihematomal edema expansion predicts outcome after intracerebral hemorrhage. *Critical care medicine*. 2016;44:790-797

27. Fu Y, Liu Q, Anrather J, Shi FD. Immune interventions in stroke. *Nat Rev Neurol*. 2015;11:524-535

28. Macrez R, Ali C, Toutirais O, Le Mauff B, Defer G, Dirnagl U, Vivien D. Stroke and the immune system: From pathophysiology to new therapeutic strategies. *Lancet Neurol*. 2011;10:471-480

29. Iadecola C, Anrather J. The immunology of stroke: From mechanisms to translation. *Nature medicine*. 2011;17:796-808

30. Wang J. Preclinical and clinical research on inflammation after intracerebral hemorrhage. *Progress in neurobiology*. 2010;92:463-477

31. Wang X, Arima H, Yang J, Zhang S, Wu G, Woodward M, Munoz-Venturelli P, Lavados PM, Stapf C, Robinson T, Heeley E, Delcourt C, Lindley RI, Parsons M, Chalmers J, Anderson CS, Investigators I. Mannitol and outcome in intracerebral hemorrhage: Propensity score and multivariable intensive blood pressure reduction in acute cerebral hemorrhage trial 2 results. *Stroke*. 2015;46:2762-2767

32. Misra UK, Kalita J, Ranjan P, Mandal SK. Mannitol in intracerebral hemorrhage: A randomized controlled study. *Journal of the neurological sciences*. 2005;234:41-45

33. Jiang B, Li L, Chen Q, Tao Y, Yang L, Zhang B, Zhang JH, Feng H, Chen Z, Tang J, Zhu G. Role of glibenclamide in brain injury after intracerebral hemorrhage. *Translational stroke research*. 2017;8:183-193

34. Fu Y, Hao J, Zhang N, Ren L, Sun N, Li YJ, Yan Y, Huang D, Yu C, Shi FD. Fingolimod for the treatment of intracerebral hemorrhage: A 2-arm proof-of-concept study. *JAMA Neurol*. 2014;71:1092-1101

35. Chang CF, Goods BA, Askenase MH, Hammond MD, Renfroe SC, Steinschneider AF, Landreneau MJ, Ai Y, Beatty HE, da Costa LHA, Mack M, Sheth KN, Greer DM, Huttner A, Coman D, Hyder F, Ghosh S, Rothlin CV, Love JC, Sansing LH. Erythrocyte efferocytosis modulates macrophages towards recovery after intracerebral hemorrhage. *J Clin Invest*. 2018;128:607-624

36. Xiong XY, Liu L, Wang FX, Yang YR, Hao JW, Wang PF, Zhong Q, Zhou K, Xiong A, Zhu WY, Zhao T, Meng ZY, Wang YC, Gong QW, Liao MF, Wang J, Yang QW. Toll-like receptor 4/myd88-mediated signaling of hepcidin expression causing brain iron accumulation, oxidative injury, and cognitive impairment after intracerebral hemorrhage. *Circulation*. 2016;134:1025-1038

37. Wu J, Hua Y, Keep RF, Schallert T, Hoff JT, Xi G. Oxidative brain injury from extravasated erythrocytes after intracerebral hemorrhage. *Brain Res*. 2002;953:45-52

38. Zhao XR, Gonzales N, Aronowski J. Pleiotropic role of ppargamma in intracerebral hemorrhage: An intricate system involving nrf2, rxr, and nf-kappab. *CNS neuroscience & therapeutics*. 2015;21:357-366

39. Gonzales NR, Shah J, Sangha N, Sosa L, Martinez R, Shen L, Kasam M, Morales MM, Hossain MM, Barreto AD, Savitz SI, Lopez G, Misra V, Wu TC, El Khoury R, Sarraj A, Sahota P, Hicks W, Acosta I, Sline MR, Rahbar MH, Zhao X, Aronowski J, Grotta JC. Design of a prospective, dose-escalation study evaluating the safety of pioglitazone for hematoma resolution in intracerebral hemorrhage (shrinc). *International journal of stroke : official journal of the International Stroke Society*. 2013;8:388-396

40. Morotti A, Boulouis G, Romero JM, Brouwers HB, Jessel MJ, Vashkevich A, Schwab K, Afzal MR, Cassarly C, Greenberg SM, Martin RH, Qureshi AI, Rosand J, Goldstein JN, Atach, II, investigators N. Blood pressure reduction and noncontrast ct markers of intracerebral hemorrhage expansion. *Neurology*. 2017;89:548-554

41. Morotti A, Brouwers HB, Romero JM, Jessel MJ, Vashkevich A, Schwab K, Afzal MR, Cassarly C, Greenberg SM, Martin RH, Qureshi AI, Rosand J, Goldstein JN,

Antihypertensive Treatment of Acute Cerebral H, II, Neurological Emergencies Treatment Trials I. Intensive blood pressure reduction and spot sign in intracerebral hemorrhage: A secondary analysis of a randomized clinical trial. *JAMA Neurol*. 2017;74:950-960

42. Moullaali TJ, Wang X, Woodhouse LJ, Law ZK, Delcourt C, Sprigg N, Krishnan K, Robinson TG, Wardlaw JM, Al-Shahi Salman R, Berge E, Sandset EC, Anderson CS, Bath PM, Investigators B. Lowering blood pressure after acute intracerebral haemorrhage: Protocol for a systematic review and meta-analysis using individual patient data from randomised controlled trials participating in the blood pressure in acute stroke collaboration (basc). *BMJ Open*. 2019;9:e030121

43. Leasure AC, Qureshi AI, Murthy SB, Kamel H, Goldstein JN, Walsh KB, Woo D, Shi FD, Huttner HB, Ziai WC, Hanley DF, Matouk CC, Sansing LH, Falcone GJ, Sheth KN. Intensive blood pressure reduction and perihematomal edema expansion in deep intracerebral hemorrhage. *Stroke*. 2019;50:2016-2022

44. Hanley DF, Thompson RE, Muschelli J, Rosenblum M, McBee N, Lane K, Bistran-Hall AJ, Mayo SW, Keyl P, Gandhi D, Morgan TC, Ullman N, Mould WA, Carhuapoma JR, Kase C, Ziai W, Thompson CB, Yenokyan G, Huang E, Broaddus WC, Graham RS, Aldrich EF, Dodd R, Wijman C, Caron JL, Huang J, Camarata P, Mendelow AD, Gregson B, Janis S, Vespa P, Martin N, Awad I, Zuccarello M, Investigators M. Safety and efficacy of minimally invasive surgery plus alteplase in intracerebral haemorrhage evacuation (mistie): A randomised, controlled, open-label, phase 2 trial. *Lancet Neurol*. 2016;15:1228-1237

45. Hanley DF, Lane K, McBee N, Ziai W, Tuhrim S, Lees KR, Dawson J, Gandhi D, Ullman N, Mould WA, Mayo SW, Mendelow AD, Gregson B, Butcher K, Vespa P, Wright DW, Kase CS, Carhuapoma JR, Keyl PM, Diener-West M, Muschelli J, Betz JF, Thompson CB, Sugar EA, Yenokyan G, Janis S, John S, Harnof S, Lopez GA, Aldrich EF, Harrigan MR, Ansari S, Jallo J, Caron JL, LeDoux D, Adeoye O, Zuccarello M, Adams HP, Jr., Rosenblum M, Thompson RE, Awad IA, Investigators CI. Thrombolytic removal of intraventricular haemorrhage in treatment of severe stroke: Results of the randomised, multicentre, multiregion, placebo-controlled clear iii trial. *Lancet*. 2017;389:603-611

46. Zeng L, Tan L, Li H, Zhang Q, Li Y, Guo J. Deferoxamine therapy for intracerebral hemorrhage: A systematic review. *PloS one*. 2018;13:e0193615

47. Fayad PB, Awad IA. Surgery for intracerebral hemorrhage. *Neurology*. 1998;51:S69-73

48. Mendelow AD, Gregson BA, Fernandes HM, Murray GD, Teasdale GM, Hope DT, Karimi A, Shaw MD, Barer DH, investigators S. Early surgery versus initial conservative treatment

in patients with spontaneous supratentorial intracerebral haematomas in the international surgical trial in intracerebral haemorrhage (stich): A randomised trial. *Lancet*. 2005;365:387-397

49. Mendelow AD, Gregson BA, Rowan EN, Murray GD, Gholkar A, Mitchell PM, Investigators SI. Early surgery versus initial conservative treatment in patients with spontaneous supratentorial lobar intracerebral haematomas (stich ii): A randomised trial. *Lancet*. 2013;382:397-408

50. Mould WA, Carhuapoma JR, Muschelli J, Lane K, Morgan TC, McBee NA, Bistran-Hall AJ, Ullman NL, Vespa P, Martin NA, Awad I, Zuccarello M, Hanley DF, Investigators M. Minimally invasive surgery plus recombinant tissue-type plasminogen activator for intracerebral hemorrhage evacuation decreases perihematomal edema. *Stroke*. 2013;44:627-634

51. Hanley DF, Thompson RE, Rosenblum M, Yenokyan G, Lane K, McBee N, Mayo SW, Bistran-Hall AJ, Gandhi D, Mould WA, Ullman N, Ali H, Carhuapoma JR, Kase CS, Lees KR, Dawson J, Wilson A, Betz JF, Sugar EA, Hao Y, Avadhani R, Caron JL, Harrigan MR, Carlson AP, Bulters D, LeDoux D, Huang J, Cobb C, Gupta G, Kitagawa R, Chicoine MR, Patel H, Dodd R, Camarata PJ, Wolfe S, Stadnik A, Money PL, Mitchell P, Sarabia R, Harnof S, Barzo P, Unterberg A, Teitelbaum JS, Wang W, Anderson CS, Mendelow AD, Gregson B, Janis S, Vespa P, Ziai W, Zuccarello M, Awad IA, Investigators MI. Efficacy and safety of minimally invasive surgery with thrombolysis in intracerebral haemorrhage evacuation (mistie iii): A randomised, controlled, open-label, blinded endpoint phase 3 trial. *Lancet*. 2019;393:1021-1032

52. Brouwers HB, Greenberg SM. Hematoma expansion following acute intracerebral hemorrhage. *Cerebrovascular diseases*. 2013;35:195-201

53. Edlow BL, Bove RM, Viswanathan A, Greenberg SM, Silverman SB. The pattern and pace of hyperacute hemorrhage expansion. *Neurocritical care*. 2012;17:250-254

54. Schlunk F, Greenberg SM. The pathophysiology of intracerebral hemorrhage formation and expansion. *Translational stroke research*. 2015;6:257-263

55. Adeoye O, Broderick JP. Advances in the management of intracerebral hemorrhage. *Nat Rev Neurol*. 2010;6:593-601

56. Qureshi AI, Mendelow AD, Hanley DF. Intracerebral haemorrhage. *Lancet*. 2009;373:1632-1644

57. Mracsko E, Javidi E, Na SY, Kahn A, Liesz A, Veltkamp R. Leukocyte invasion of the brain after experimental intracerebral hemorrhage in mice. *Stroke*. 2014;45:2107-2114

58. Zhao X, Sun G, Zhang J, Strong R, Song W, Gonzales N, Grotta JC, Aronowski J. Hematoma resolution as a target for intracerebral hemorrhage treatment: Role for peroxisome proliferator-activated receptor gamma in microglia/macrophages. *Annals of neurology*. 2007;61:352-362

59. Lan X, Han X, Li Q, Yang QW, Wang J. Modulators of microglial activation and polarization after intracerebral haemorrhage. *Nat Rev Neurol*. 2017;13:420-433

60. Aronowski J, Zhao X. Molecular pathophysiology of cerebral hemorrhage: Secondary brain injury. *Stroke*. 2011;42:1781-1786

61. Jabri B, Abadie V. Il-15 functions as a danger signal to regulate tissue-resident t cells and tissue destruction. *Nature reviews. Immunology*. 2015;15:771-783

62. Mishra A, Sullivan L, Caligiuri MA. Molecular pathways: Interleukin-15 signaling in health and in cancer. *Clinical cancer research : an official journal of the American Association for Cancer Research*. 2014;20:2044-2050

63. Park JY, Lee SH, Yoon SR, Park YJ, Jung H, Kim TD, Choi I. Il-15-induced il-10 increases the cytolytic activity of human natural killer cells. *Molecules and cells*. 2011;32:265-272

64. McInnes IB, Leung BP, Sturrock RD, Field M, Liew FY. Interleukin-15 mediates t cell-dependent regulation of tumor necrosis factor-alpha production in rheumatoid arthritis. *Nature medicine*. 1997;3:189-195

65. Sakai T, Kusugami K, Nishimura H, Ando T, Yamaguchi T, Ohsuga M, Ina K, Enomoto A, Kimura Y, Yoshikai Y. Interleukin 15 activity in the rectal mucosa of inflammatory bowel disease. *Gastroenterology*. 1998;114:1237-1243

66. Gomez-Nicola D, Valle-Argos B, Pita-Thomas DW, Nieto-Sampedro M. Interleukin 15 expression in the cns: Blockade of its activity prevents glial activation after an inflammatory injury. *Glia*. 2008;56:494-505

67. Gomez-Nicola D, Valle-Argos B, Nieto-Sampedro M. Blockade of il-15 activity inhibits microglial activation through the nfkappab, p38, and erk1/2 pathways, reducing cytokine and chemokine release. *Glia*. 2010;58:264-276

68. Wu X, Pan W, He Y, Hsuchou H, Kastin AJ. Cerebral interleukin-15 shows upregulation and beneficial effects in experimental autoimmune encephalomyelitis. *Journal of neuroimmunology*. 2010;223:65-72

69. Li Z, Han J, Ren H, Ma CG, Shi FD, Liu Q, Li M. Astrocytic interleukin-15 reduces pathology of neuromyelitis optica in mice. *Frontiers in immunology*. 2018;9:523

70. Roy-O'Reilly M, McCullough LD. Astrocytes fuel the fire of lymphocyte toxicity after stroke. *Proceedings of the National Academy of Sciences of the United States of America*. 2017;114:425-427

71. Zhao Q, Yan T, Li L, Chopp M, Venkat P, Qian Y, Li R, Wu R, Li W, Lu M, Zhang T, Chen J. Immune response mediates cardiac dysfunction after traumatic brain injury. *J Neurotrauma*. 2019;36:619-629

72. Benakis C, Brea D, Caballero S, Faraco G, Moore J, Murphy M, Sita G, Racchumi G, Ling L, Pamer EG, Iadecola C, Anrather J. Commensal microbiota affects ischemic stroke outcome by regulating intestinal gammadelta t cells. *Nature medicine*. 2016;22:516-523

73. Wong CH, Jenne CN, Lee WY, Leger C, Kubes P. Functional innervation of hepatic inkt cells is immunosuppressive following stroke. *Science*. 2011;334:101-105

74. Li W, Li L, Chopp M, Venkat P, Zacharek A, Chen Z, Landschoot-Ward J, Yan T, Chen J. Intracerebral hemorrhage induces cardiac dysfunction in mice without primary cardiac disease. *Front Neurol*. 2018;9:965

75. Yan T, Chen Z, Chopp M, Venkat P, Zacharek A, Li W, Shen Y, Wu R, Li L, Landschoot-Ward J, Lu M, Hank KH, Zhang J, Chen J. Inflammatory responses mediate brain-heart interaction after ischemic stroke in adult mice. *J Cereb Blood Flow Metab*. 2018:271678X18813317

76. Singh V, Roth S, Llovera G, Sadler R, Garzetti D, Stecher B, Dichgans M, Liesz A. Microbiota dysbiosis controls the neuroinflammatory response after stroke. *J Neurosci*. 2016;36:7428-7440

77. Loftspring MC, McDole J, Lu A, Clark JF, Johnson AJ. Intracerebral hemorrhage leads to infiltration of several leukocyte populations with concomitant pathophysiological changes. *J Cereb Blood Flow Metab*. 2009;29:137-143

78. Hammond MD, Taylor RA, Mullen MT, Ai Y, Aguila HL, Mack M, Kasner SE, McCullough LD, Sansing LH. Ccr2+ ly6c(hi) inflammatory monocyte recruitment exacerbates acute disability following intracerebral hemorrhage. *J Neurosci*. 2014;34:3901-3909

79. Zhao X, Grotta J, Gonzales N, Aronowski J. Hematoma resolution as a therapeutic target: The role of microglia/macrophages. *Stroke*. 2009;40:S92-94

80. Vaibhav K, Braun M, Khan MB, Fatima S, Saad N, Shankar A, Khan ZT, Harris RBS, Yang Q, Huo Y, Arbab AS, Giri S, Alleyne CH, Jr., Vender JR, Hess DC, Baban B, Hoda MN, Dhandapani KM. Remote ischemic post-conditioning promotes hematoma resolution via ampk-dependent immune regulation. *J Exp Med*. 2018;215:2636-2654

81. Chang CF, Wan J, Li Q, Renfroe SC, Heller NM, Wang J. Alternative activation-skewed microglia/macrophages promote hematoma resolution in experimental intracerebral hemorrhage. *Neurobiol Dis*. 2017;103:54-69

82. Wei Q, Frenette PS. Niches for hematopoietic stem cells and their progeny. *Immunity*. 2018;48:632-648

83. Orkin SH, Zon LI. Hematopoiesis: An evolving paradigm for stem cell biology. *Cell*. 2008;132:631-644

84. Ito K, Frenette PS. Hsc contribution in making steady-state blood. *Immunity*. 2016;45:464-466

85. Laurenti E, Gottgens B. From haematopoietic stem cells to complex differentiation landscapes. *Nature*. 2018;553:418-426

86. Boettcher S, Manz MG. Regulation of inflammation- and infection-driven hematopoiesis. *Trends in immunology*. 2017;38:345-357

87. Janssen WJ, Bratton DL, Jakubzick CV, Henson PM. Myeloid cell turnover and clearance. *Microbiol Spectr*. 2016;4

88. Leuschner F, Rauch PJ, Ueno T, Gorbatov R, Marinelli B, Lee WW, Dutta P, Wei Y, Robbins C, Iwamoto Y, Sena B, Chudnovskiy A, Panizzi P, Keliher E, Higgins JM, Libby P, Moskowitz MA, Pittet MJ, Swirski FK, Weissleder R, Nahrendorf M. Rapid monocyte kinetics in acute myocardial infarction are sustained by extramedullary monocytopoiesis. *J Exp Med*. 2012;209:123-137

89. Mendelson A, Frenette PS. Hematopoietic stem cell niche maintenance during homeostasis and regeneration. *Nature medicine*. 2014;20:833-846

90. King KY, Goodell MA. Inflammatory modulation of hscs: Viewing the hsc as a foundation for the immune response. *Nature reviews. Immunology*. 2011;11:685-692

91. Hanoun M, Maryanovich M, Arnal-Estape A, Frenette PS. Neural regulation of hematopoiesis, inflammation, and cancer. *Neuron*. 2015;86:360-373

92. Chapple RH, Tseng YJ, Hu T, Kitano A, Takeichi M, Hoegenauer KA, Nakada D. Lineage tracing of murine adult hematopoietic stem cells reveals active contribution to steady-state hematopoiesis. *Blood Adv*. 2018;2:1220-1228

93. Li M, Li Z, Yao Y, Jin WN, Wood K, Liu Q, Shi FD, Hao J. Astrocyte-derived interleukin-15 exacerbates ischemic brain injury via propagation of cellular immunity. *Proceedings of the National Academy of Sciences of the United States of America*. 2017;114:E396-E405

94. Illanes S, Liesz A, Sun L, Dalpke A, Zorn M, Veltkamp R. Hematoma size as major modulator of the cellular immune system after experimental intracerebral hemorrhage. *Neuroscience letters*. 2011;490:170-174

95. Shi E, Shi K, Qiu S, Sheth KN, Lawton MT, Ducruet AF. Chronic inflammation, cognitive impairment, and distal brain region alteration following intracerebral hemorrhage. *FASEB journal : official publication of the Federation of American Societies for Experimental Biology*. 2019;33:9616-9626

96. Sun N, Shen Y, Han W, Shi K, Wood K, Fu Y, Hao J, Liu Q, Sheth KN, Huang D, Shi FD. Selective sphingosine-1-phosphate receptor 1 modulation attenuates experimental intracerebral hemorrhage. *Stroke*. 2016;47:1899-1906

97. Taylor RA, Chang CF, Goods BA, Hammond MD, Mac Grory B, Ai Y, Steinschneider AF, Renfroe SC, Askenase MH, McCullough LD, Kasner SE, Mullen MT, Hafler DA, Love JC, Sansing LH. Tgf-beta1 modulates microglial phenotype and promotes recovery after intracerebral hemorrhage. *J Clin Invest*. 2017;127:280-292

98. Ren H, Kong Y, Liu Z, Zang D, Yang X, Wood K, Li M, Liu Q. Selective nlrp3 (pyrin domain-containing protein 3) inflammasome inhibitor reduces brain injury after intracerebral hemorrhage. *Stroke*. 2018;49:184-192

99. Lazovic J, Basu A, Lin HW, Rothstein RP, Krady JK, Smith MB, Levison SW. Neuroinflammation and both cytotoxic and vasogenic edema are reduced in interleukin-1 type 1 receptor-deficient mice conferring neuroprotection. *Stroke*. 2005;36:2226-2231

100. Li M, Ren H, Sheth KN, Shi FD, Liu Q. A tspo ligand attenuates brain injury after intracerebral hemorrhage. *FASEB journal : official publication of the Federation of American Societies for Experimental Biology*. 2017;31:3278-3287

101. Dutta P, Sager HB, Stengel KR, Naxerova K, Courties G, Saez B, Silberstein L, Heidt T, Sebas M, Sun Y, Wojtkiewicz G, Feruglio PF, King K, Baker JN, van der Laan AM, Borodovsky A, Fitzgerald K, Hulsmans M, Hoyer F, Iwamoto Y, Vinegoni C, Brown D, Di Carli M, Libby P, Hiebert SW, Scadden DT, Swirski FK, Weissleder R, Nahrendorf M.

Myocardial infarction activates ccr2(+) hematopoietic stem and progenitor cells. *Cell Stem Cell*. 2015;16:477-487

102. Yang X, Ren H, Wood K, Li M, Qiu S, Shi FD, Ma C, Liu Q. Depletion of microglia augments the dopaminergic neurotoxicity of mptp. *FASEB journal : official publication of the Federation of American Societies for Experimental Biology*. 2018;32:3336-3345

103. Jin WN, Shi SX, Li Z, Li M, Wood K, Gonzales RJ, Liu Q. Depletion of microglia exacerbates postischemic inflammation and brain injury. *J Cereb Blood Flow Metab*. 2017;37:2224-2236

104. Li M, Li Z, Ren H, Jin WN, Wood K, Liu Q, Sheth KN, Shi FD. Colony stimulating factor 1 receptor inhibition eliminates microglia and attenuates brain injury after intracerebral hemorrhage. *J Cereb Blood Flow Metab*. 2017;37:2383-2395

105. Jin WN, Yang X, Li Z, Li M, Shi SX, Wood K, Liu Q, Fu Y, Han W, Xu Y, Shi FD, Liu Q. Non-invasive tracking of cd4+ t cells with a paramagnetic and fluorescent nanoparticle in brain ischemia. *J Cereb Blood Flow Metab*. 2016;36:1464-1476

106. Shi SX, Li YJ, Shi K, Wood K, Ducruet AF, Liu Q. Il (interleukin)-15 bridges astrocyte-microglia crosstalk and exacerbates brain injury following intracerebral hemorrhage. *Stroke*. 2020;51:967-974

107. Morotti A, Phuah CL, Anderson CD, Jessel MJ, Schwab K, Ayres AM, Pezzini A, Padovani A, Gurol ME, Viswanathan A, Greenberg SM, Goldstein JN, Rosand J. Leukocyte count and intracerebral hemorrhage expansion. *Stroke*. 2016;47:1473-1478

108. Tapia-Perez JH, Karagianis D, Zilke R, Koufuglou V, Bondar I, Schneider T. Assessment of systemic cellular inflammatory response after spontaneous intracerebral hemorrhage. *Clinical neurology and neurosurgery*. 2016;150:72-79

109. Gusdon AM, Gialdini G, Kone G, Baradaran H, Merkler AE, Mangat HS, Navi BB, Iadecola C, Gupta A, Kamel H, Murthy SB. Neutrophil-lymphocyte ratio and perihematomal edema growth in intracerebral hemorrhage. *Stroke*. 2017;48:2589-2592

110. Vasamsetti SB, Florentin J, Coppin E, Stiekema LCA, Zheng KH, Nisar MU, Sembrat J, Levinthal DJ, Rojas M, Stroes ESG, Kim K, Dutta P. Sympathetic neuronal activation triggers myeloid progenitor proliferation and differentiation. *Immunity*. 2018;49:93-106 e107

111. Dutta P, Courties G, Wei Y, Leuschner F, Gorbatov R, Robbins CS, Iwamoto Y, Thompson B, Carlson AL, Heidt T, Majmudar MD, Lasitschka F, Etzrodt M, Waterman P, Waring MT, Chicoine AT, van der Laan AM, Niessen HW, Piek JJ, Rubin BB, Butany J, Stone JR,

Katus HA, Murphy SA, Morrow DA, Sabatine MS, Vinegoni C, Moskowitz MA, Pittet MJ, Libby P, Lin CP, Swirski FK, Weissleder R, Nahrendorf M. Myocardial infarction accelerates atherosclerosis. *Nature*. 2012;487:325-329

112. Guilliams M, Mildner A, Yona S. Developmental and functional heterogeneity of monocytes. *Immunity*. 2018;49:595-613

113. Trompette A, Gollwitzer ES, Pattaroni C, Lopez-Mejia IC, Riva E, Pernot J, Ubags N, Fajas L, Nicod LP, Marsland BJ. Dietary fiber confers protection against flu by shaping ly6c(-) patrolling monocyte hematopoiesis and cd8(+) t cell metabolism. *Immunity*. 2018;48:992-1005 e1008

114. Wang L, Yang L, Filippi MD, Williams DA, Zheng Y. Genetic deletion of cdc42gap reveals a role of cdc42 in erythropoiesis and hematopoietic stem/progenitor cell survival, adhesion, and engraftment. *Blood*. 2006;107:98-105

115. Yang L, Wang L, Kalfa TA, Cancelas JA, Shang X, Pushkaran S, Mo J, Williams DA, Zheng Y. Cdc42 critically regulates the balance between myelopoiesis and erythropoiesis. *Blood*. 2007;110:3853-3861

116. Florian MC, Nattamai KJ, Dorr K, Marka G, Uberle B, Vas V, Eckl C, Andra I, Schiemann M, Oostendorp RA, Scharffetter-Kochanek K, Kestler HA, Zheng Y, Geiger H. A canonical to non-canonical wnt signalling switch in haematopoietic stem-cell ageing. *Nature*. 2013;503:392-396

117. Yang L, Wang L, Geiger H, Cancelas JA, Mo J, Zheng Y. Rho gtpase cdc42 coordinates hematopoietic stem cell quiescence and niche interaction in the bone marrow. *Proceedings of the National Academy of Sciences of the United States of America*. 2007;104:5091-5096

118. Sui W, Li H, Yang Y, Jing X, Xue F, Cheng J, Dong M, Zhang M, Pan H, Chen Y, Zhang Y, Zhou Q, Shi W, Wang X, Zhang H, Zhang C, Zhang Y, Cao Y. Bladder drug mirabegron exacerbates atherosclerosis through activation of brown fat-mediated lipolysis. *Proceedings of the National Academy of Sciences of the United States of America*. 2019;116:10937-10942

119. Calmasini FB, de Oliveira MG, Alexandre EC, da Silva FH, da Silva CPV, Candido TZ, Antunes E, Monica FZ. Long-term treatment with the beta-3 adrenoceptor agonist, mirabegron ameliorates detrusor overactivity and restores cyclic adenosine monophosphate (camp) levels in obese mice. *Neurourol Urodyn*. 2017;36:1511-1518

120. Grill B, Schrader JW. Activation of rac-1, rac-2, and cdc42 by hemopoietic growth factors or cross-linking of the b-lymphocyte receptor for antigen. *Blood*. 2002;100:3183-3192

121. Ransohoff RM, Brown MA. Innate immunity in the central nervous system. *J Clin Invest*. 2012;122:1164-1171

122. Khakh BS, Sofroniew MV. Diversity of astrocyte functions and phenotypes in neural circuits. *Nature neuroscience*. 2015;18:942-952

123. Perera LP, Goldman CK, Waldmann TA. Il-15 induces the expression of chemokines and their receptors in t lymphocytes. *Journal of immunology*. 1999;162:2606-2612

124. McInnes IB, al-Mughales J, Field M, Leung BP, Huang FP, Dixon R, Sturrock RD, Wilkinson PC, Liew FY. The role of interleukin-15 in t-cell migration and activation in rheumatoid arthritis. *Nature medicine*. 1996;2:175-182

125. Galea J, Ogungbenro K, Hulme S, Patel H, Scarth S, Hoadley M, Illingworth K, McMahon CJ, Tzerakis N, King AT, Vail A, Hopkins SJ, Rothwell N, Tyrrell P. Reduction of inflammation after administration of interleukin-1 receptor antagonist following aneurysmal subarachnoid hemorrhage: Results of the subcutaneous interleukin-1ra in sah (scil-sah) study. *Journal of neurosurgery*. 2018;128:515-523

126. Zhang F, Ren Y, Shi Y, Fu W, Tao C, Li X, Yang M, You C, Xin T. Predictive ability of admission neutrophil to lymphocyte ratio on short-term outcome in patients with spontaneous cerebellar hemorrhage. *Medicine (Baltimore)*. 2019;98:e16120

127. Qi H, Wang D, Deng X, Pang X. Lymphocyte-to-monocyte ratio is an independent predictor for neurological deterioration and 90-day mortality in spontaneous intracerebral hemorrhage. *Med Sci Monit*. 2018;24:9282-9291

128. Adeoye O, Walsh K, Woo JG, Haverbusch M, Moomaw CJ, Broderick JP, Kissela BM, Kleindorfer D, Flaherty ML, Woo D. Peripheral monocyte count is associated with case fatality after intracerebral hemorrhage. *J Stroke Cerebrovasc Dis*. 2014;23:e107-111

129. Walsh KB, Sekar P, Langefeld CD, Moomaw CJ, Elkind MS, Boehme AK, James ML, Osborne J, Sheth KN, Woo D, Adeoye O. Monocyte count and 30-day case fatality in intracerebral hemorrhage. *Stroke*. 2015;46:2302-2304

130. Walsh KB, Zhang X, Zhu X, Wohleb E, Woo D, Lu L, Adeoye O. Intracerebral hemorrhage induces monocyte-related gene expression within six hours: Global transcriptional profiling in swine ich. *Metab Brain Dis*. 2019;34:763-774

131. Wheeler MA, Jaronen M, Covacu R, Zandee SEJ, Scalisi G, Rothhammer V, Tjon EC, Chao CC, Kenison JE, Blain M, Rao VTS, Hewson P, Barroso A, Gutierrez-Vazquez C,

Prat A, Antel JP, Hauser R, Quintana FJ. Environmental control of astrocyte pathogenic activities in cns inflammation. *Cell*. 2019;176:581-596 e518